Structural Diversity, Photo-physical and Magnetic Properties of Dimeric to 1D Polymeric Coordination Polymers of Lighter Lanthanide(III) Dinitrobenzoates

Amanpreet Kaur Jassal,[a] Balkaran Singh Sran,[a] Yan Suffren,[b] Kevin Bernot,[b] Fabrice Pointillart*,[c] Olivier Cador*,[c] Geeta Hundal*[a]

[a] *Department of Chemistry, UGC sponsored centre of advance studies-II, Guru Nanak Dev University, Amritsar-143005, Punjab, India.*

[b] *Institut des Sciences Chimiques de Rennes, UMR 6226 CNRS-Université de Rennes 1, 263 Avenue du Général Leclerc, 35042 Rennes Cedex, France*

[c] *Institut des Sciences Chimiques de Rennes, UMR CNRS 6226, INSA Rennes, 20 Avenue des buttes de Coesmes, 35708 Rennes, France.*

Fabrice.pointillart@univ-rennes1.fr; Olivier.cador@univ-rennes1.fr; **geetahundal@yahoo.com**;

ELECTRONIC SUPPLEMENTARY INFORMATION

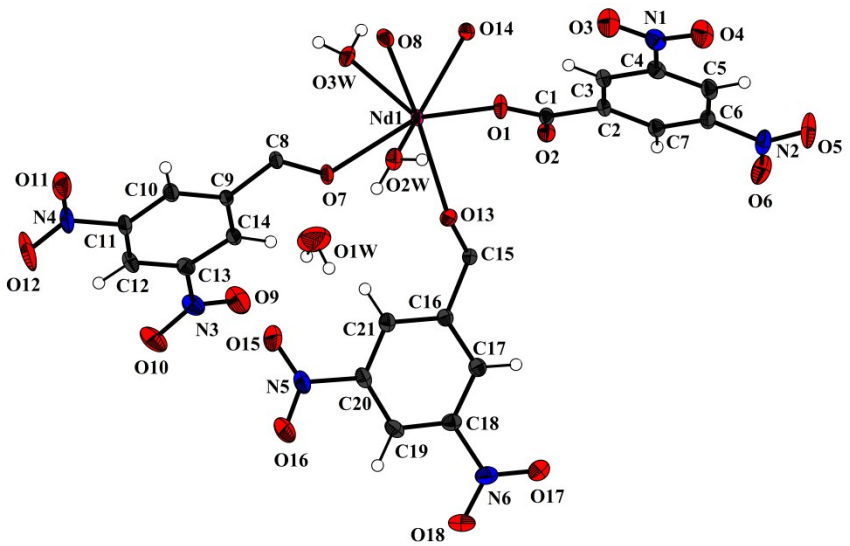

Figure S1. ORTEP showing asymmetric unit of complex **1** with 30 % probability.

Discussion of H-Bonding in Complex 1 Hydrogen atoms of lattice water O1W are H-bonded to coordinated water O2W with a distance O2W-H22W···O1W = 2.009(3) Å. Proton H12W of lattice water O2W is H-bonded to nitro group oxygen O17 with a distance O12W-H12W···O17 = 2.431(3) Å. These strong H-bonding interactions are further supporting the 1D H-bonded chain along *c* axis (Fig 2a). Additionally, aromatic hydrogen atoms of **L1** are also showing H-bonding with oxygens of -NO_2 groups in *bc* plane forming 2D, H-bonded network (Fig 2b).

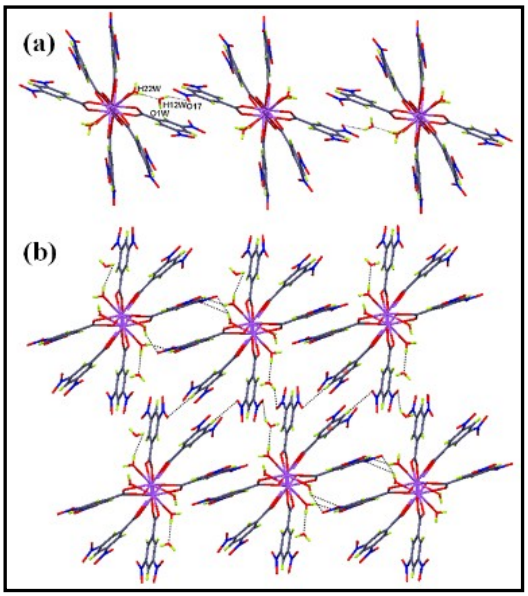

Fig S2. Showing for complex **1** (a) 1D, H-bonded chain along *c* axis, (b) 2D, H bonded network between coordinated water O1W, oxygens of –NO_2 groups and aromatic protons of **L1** in *bc* plane with channels along *a* axis.

This creates 1D channels along *a* axis which are filled by lattice water molecules (O1W) whose H-bonding interactions have been discussed earlier. The presence of a pair of coordinated water molecules and one lattice water molecule give rise to extensive hydrogen bonding and form an interesting 3D structure (Fig S2).

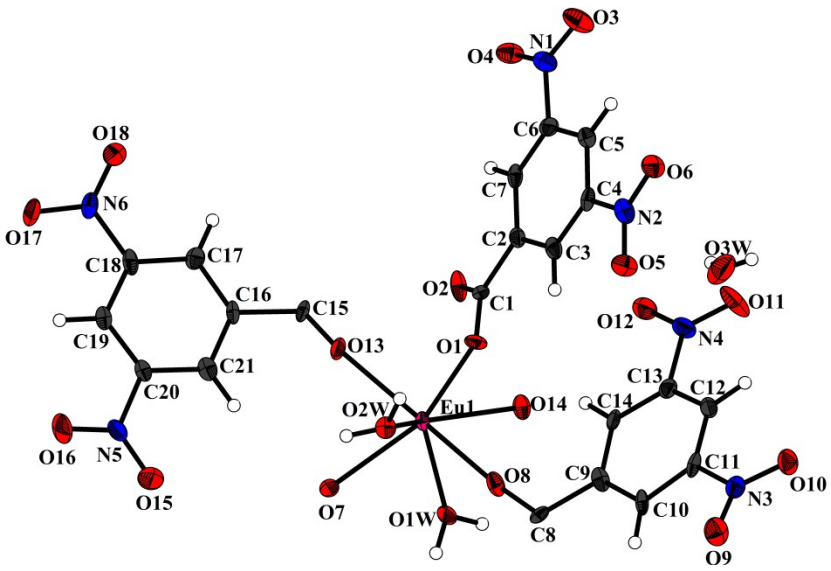

Figure S3. ORTEP showing asymmetric unit of complex **2** with 50 % probability.

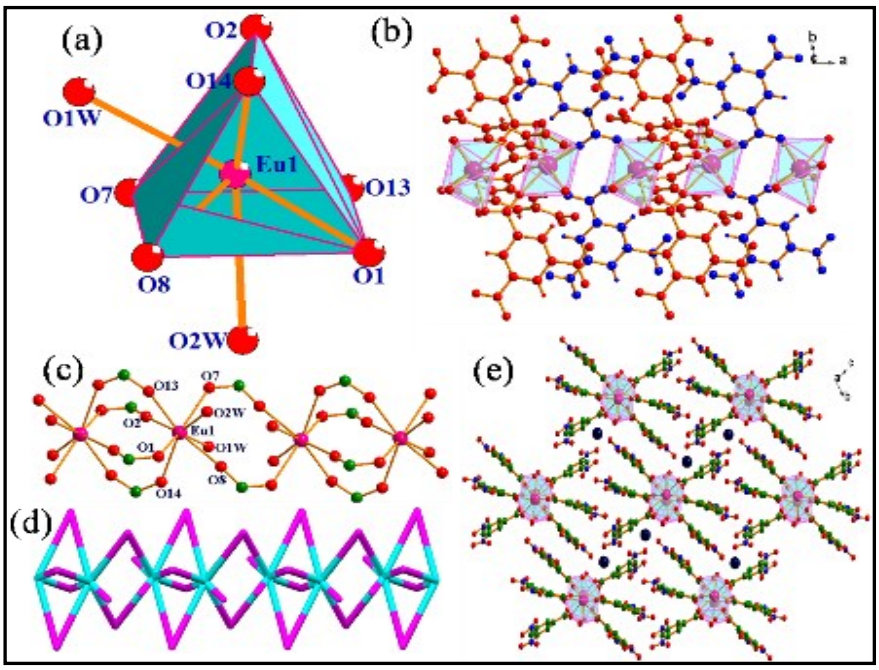

Figure S4. (a) Trigonal bicapped geometry around Eu(III) metal ion in complex **2**. (b) Polyhedral representation of 1D coordination polymer along *a* axis. (c) Ball-n-stick representation showing coordination environment around Eu(III) metal ions forming linear chain. (d) [1 0 0] chains with 2-connected uninodal net. (e) Polyhedral representation of 1D polymeric chain down the *a* axis and 3D structure due to H-bonding interactions in *bc* plane where lattice water molecules are shown in blue coloured balls.

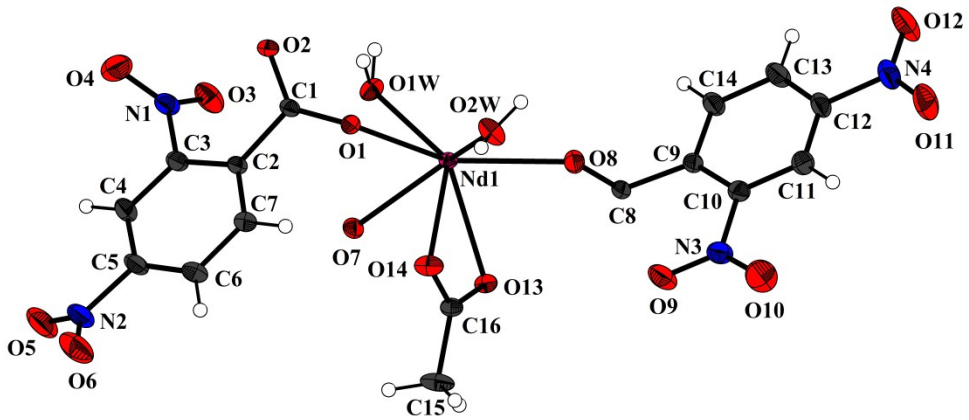

Figure S5. ORTEP showing asymmetric unit of complex **3** with 20 % probability.

Discussion of H-Bonding in Complex 3: In case of complex **3** there is strong intramolecular H-bonding interactions due to coordinated water molecules with O1W-H11W···O2W$^{\#1}$; O1W-H12W···O2W$^{\#1}$ = 2.87(3) Å (#1: -x+1,-y+2,-z) and intermolecular interactions between protons of water molecules with oxygens of nitro groups are in the range of 1.85(5) to 2.93(4) Å.

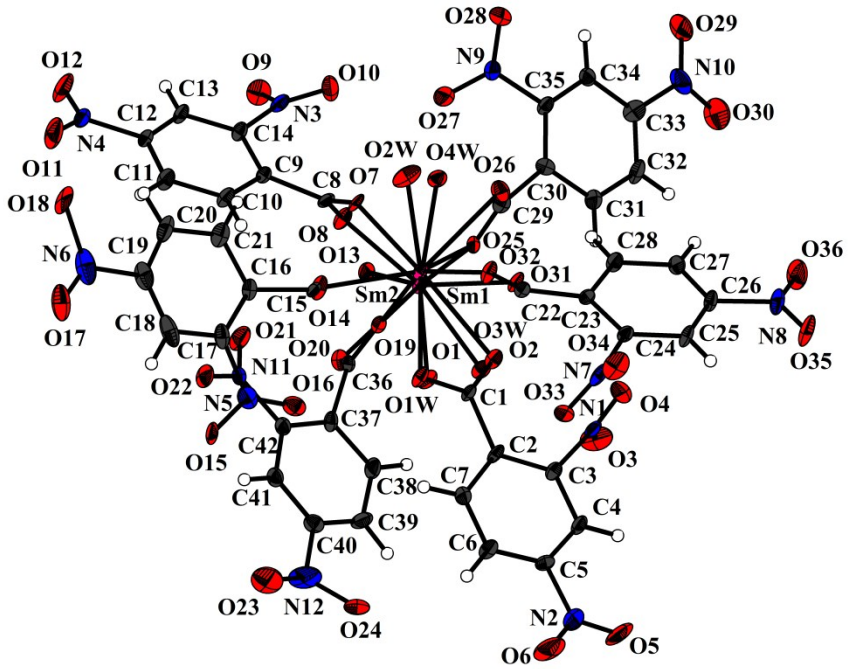

Figure S6. ORTEP showing asymmetric unit of complex **4** with 20 % probability.

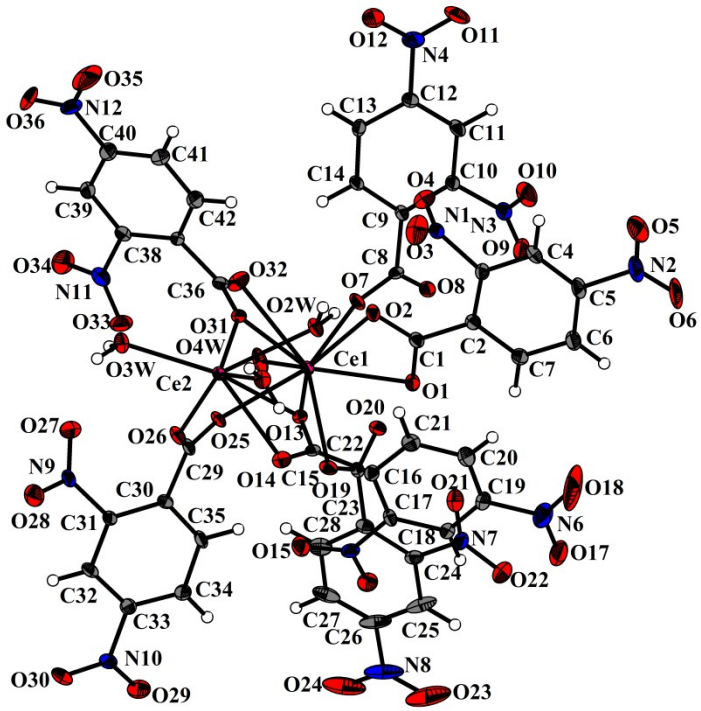

Figure S7. ORTEP showing asymmetric unit of complex **5** with 20 % probability.

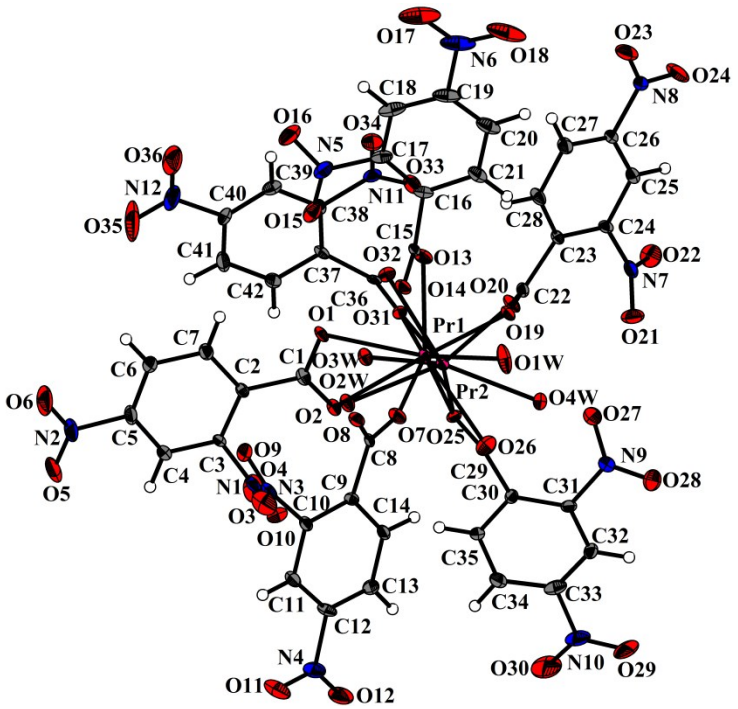

Figure S8. ORTEP showing asymmetric unit of complex **6** with 20 % probability.

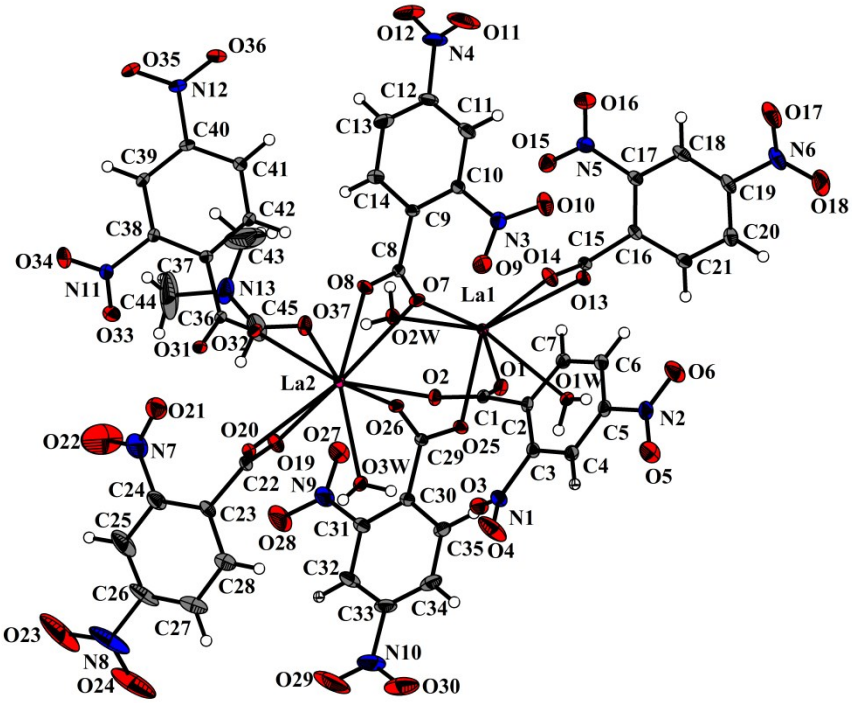

Figure S9. ORTEP showing asymmetric unit of complex **7** with 20 % probability.

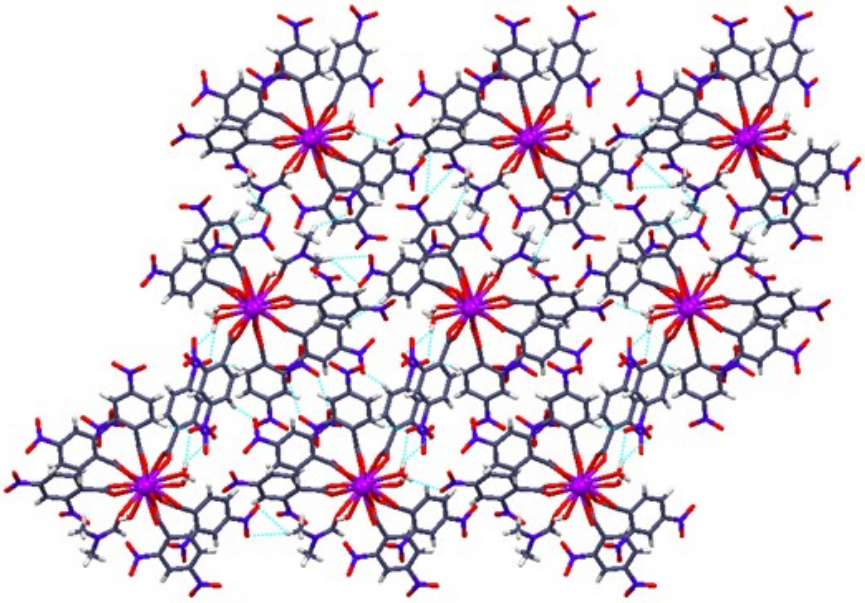

Figure S10. Intermolecular H-bonding forms 3D network as shown in *bc* plane for **Complex 7**

Discussion of H-Bonding in Complex 7: The intermolecular H-bonding interactions between hydrogen atoms of aromatic ring, coordinated water molecules with oxygens of nitro and carboxylate groups form 3D network in *bc* plane (Fig S10).

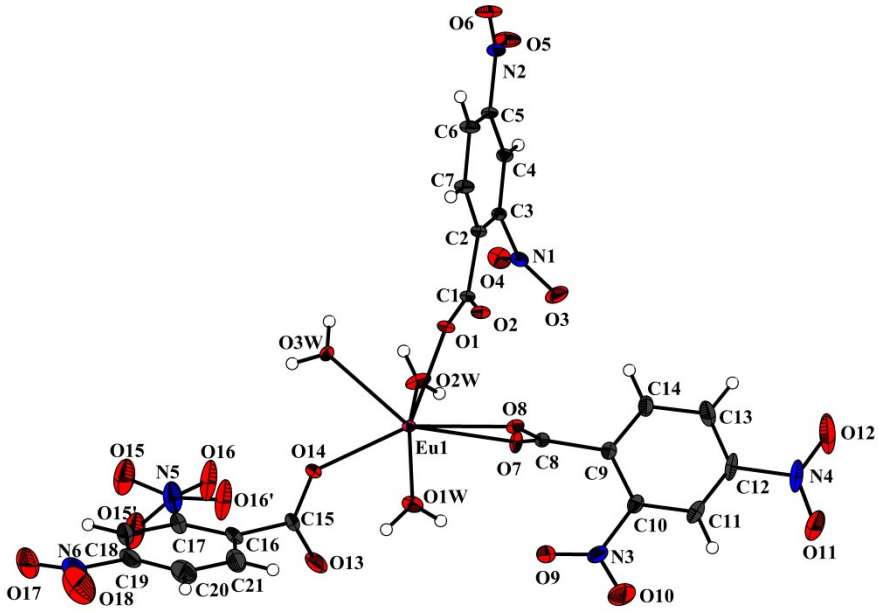

Figure S11. ORTEP showing asymmetric unit of complex **8** with 20 % probability.

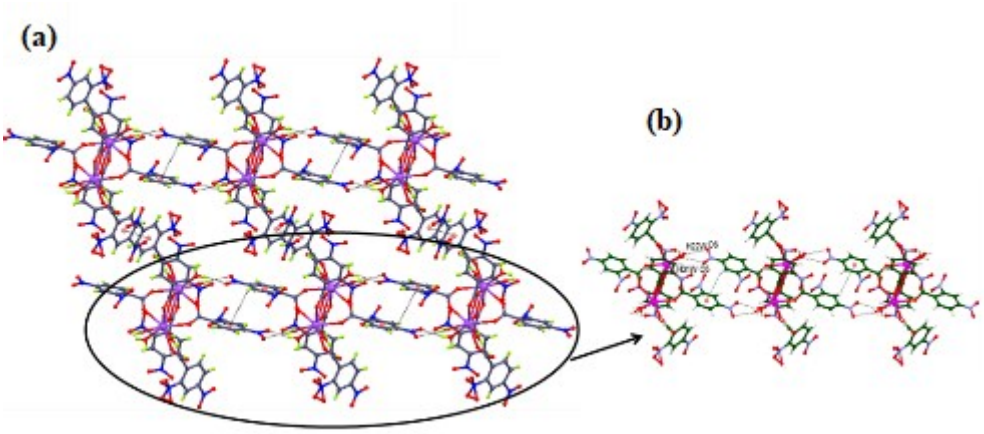

Figure S12 (a) and (b) C-H···π and H-bonding interactions between two dimeric units forming 1D chain along *b* axis whereas only weak π···π and forming 2D network in *bc* plane.

Discussion of H-Bonding and C-H···π interactions in Complex 8 : Additionally C-H···π interactions with centroid (C2-C7)···H4 distance 3.701 Å forms 1D chain along *b* axis while weak π···π interactions (centroid (C16-C21)···centroid (C16-C21) 4.150 Å) form a 2D network in *bc* plane (Fig 5(a-b)). Strong H-bonding interactions between water and nitro groups are in the range of 1.870(6) to 2.950(9) Å. The protons H22W and H31W of coordinated water are H-bonded with oxygens O6 and O5 respectively of nitro group.

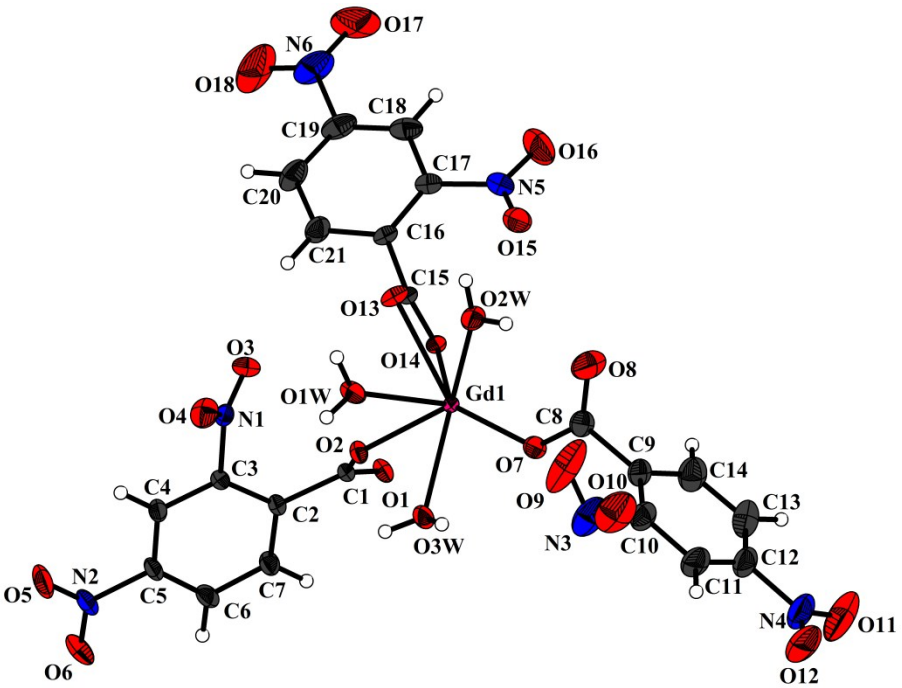

Fig S13. ORTEP showing asymmetric unit of complex **9** with 30 % probability.

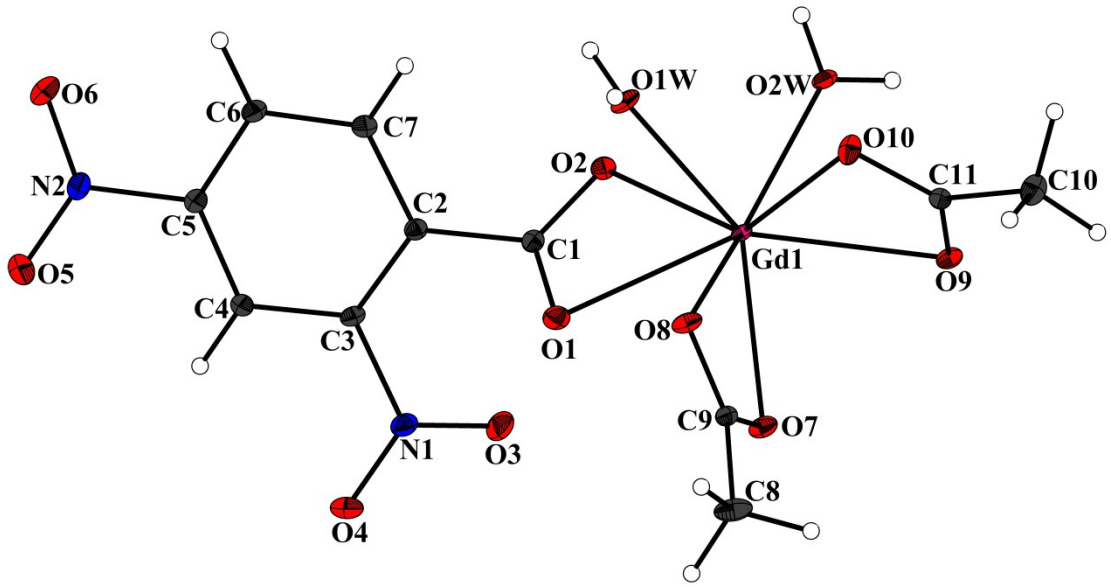

Fig S14. ORTEP showing asymmetric unit of complex **10** with 30 % probability.

Discussion of H-Bonding in Complex 10 : Strong intramolecular H-bonding interactions between water molecules and acetate groups are in the range of 1.86(3) to 2.99(2) Å. The intermolecular H-bonding interactions between protons of coordinated water and acetate group with oxygens of –NO2, –COO and acetate groups are forming corrugated chains as shown in *bc* plane **(Fig S15)**

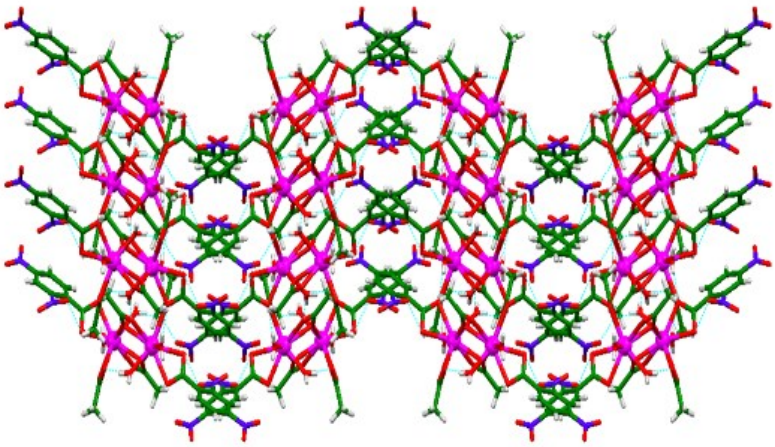

Figure S15. Intermolecular H-bonding interactions in *bc* plane in complex **10**.

IR Spectroscopy

Complexes **1-10** are studied by IR spectroscopy. In complexes **1** and **3** of Nd(III) ions, symmetric and anti-symmetric –OH stretching bands appears as a broad bands in the region of 3575-3589 cm^{-1}**.** The C-H vibrations belonging to the aromatic rings found around 3082-3112 cm^{-1} and 1404-1412 cm^{-1} for –C=C groups. The characteristic peaks of asymmetric and symmetric stretches of COO^- in the region of 1630-1643 cm^{-1} and 1535-1539 cm^{-1}, respectively. The complexes contain an aromatic N-O stretch in the region of 1346-1349 cm^{-1} and a weak bands around 583-592 cm^{-1} that are assigned to M-O vibrations. In complex **2**, the symmetric and anti-symmetric OH stretching band appears as a broad band at 3557 cm^{-1}**.** The characteristic peaks of asymmetric and symmetric stretches of COO^- at 1622 cm^{-1} and 1539 cm^{-1}, respectively. The complex contains an aromatic N-O stretch at 1342 cm^{-1}, a sp^2 C=C strong band at 1415 cm^{-1} and a weak band around 525 cm^{-1} that is assigned to M-O vibrations. In spectrum of complex **4**, a broad band centred at 3380 cm^{-1} indicating the symmetric and antisymmetric OH stretch due to H-bonding interactions. The characteristic peaks of asymmetric and symmetric stretches of COO^- in the region 1621-1542 cm^{-1}. The aromatic N-O stretch is observed at 1351 cm^{-1}. The weak band around 578 cm^{-1} is assigned to M-O vibrations. In complex **5**, OH stretching bands appears as broad bands in the region 3456 cm^{-1} and characteristic peaks of asymmetric and symmetric stretches of COO^- at 1640 cm^{-1} and

1536 cm^{-1}, respectively. The complex contains an aromatic N-O stretch at 1344 cm^{-1} and a weak band around 532 cm^{-1} and 723 cm^{-1} that are assigned to M-O vibrations. The O-H vibrations band appears as a broad band in the region 3453 cm^{-1} and characteristic peaks of asymmetric and symmetric stretches of COO^- at 1680 cm^{-1} and 1541 cm^{-1}, respectively in complex **6**. In the IR spectrum of complex **7**, **s**ymmetric and anti-symmetric OH stretching bands appears as a broad band at 3352 cm^{-1}. The characteristic peaks of asymmetric and symmetric stretches of COO^- at 1621 cm^{-1} and 1538 cm^{-1}, respectively. The complex contains an aromatic N-O stretch at 1343 cm^{-1}. The weak band around 529 cm^{-1} and 723 cm^{-1} are assigned to M-O vibrations. The complex contains an aromatic N-O stretch at 1344 cm^{-1} and a weak band around 517 cm^{-1} and 724 cm^{-1} are assigned to M-O vibrations. Complex **8** shows peaks of asymmetric and symmetric stretches of COO^- at 1630 cm^{-1} and 1531 cm^{-1}, respectively, an aromatic N-O stretch at 1352 cm^{-1} and a weak band around 567 cm^{-1} that is assigned to M-O vibrations. In complex **9**, O-H vibrations showing band at around 3337 cm^{-1}, characteristic peaks of asymmetric and symmetric stretches of COO^- around 1654 cm^{-1} and 1548 cm^{-1}, respectively. The complexes contain an aromatic N-O stretch around 1353 cm^{-1} and a weak band around 625 cm^{-1} that is assigned to M-O vibrations. The IR spectrum of the complex **10** shows a band for O-H group at 3339 cm^{-1}, characteristic peaks of asymmetric and symmetric stretches of COO^- around 1658 cm^{-1} and 1546 cm^{-1}, respectively. The complexes contain an aromatic N-O stretch around 1352 cm^{-1} and a weak band around 622 cm^{-1} that is assigned to M-O vibrations.

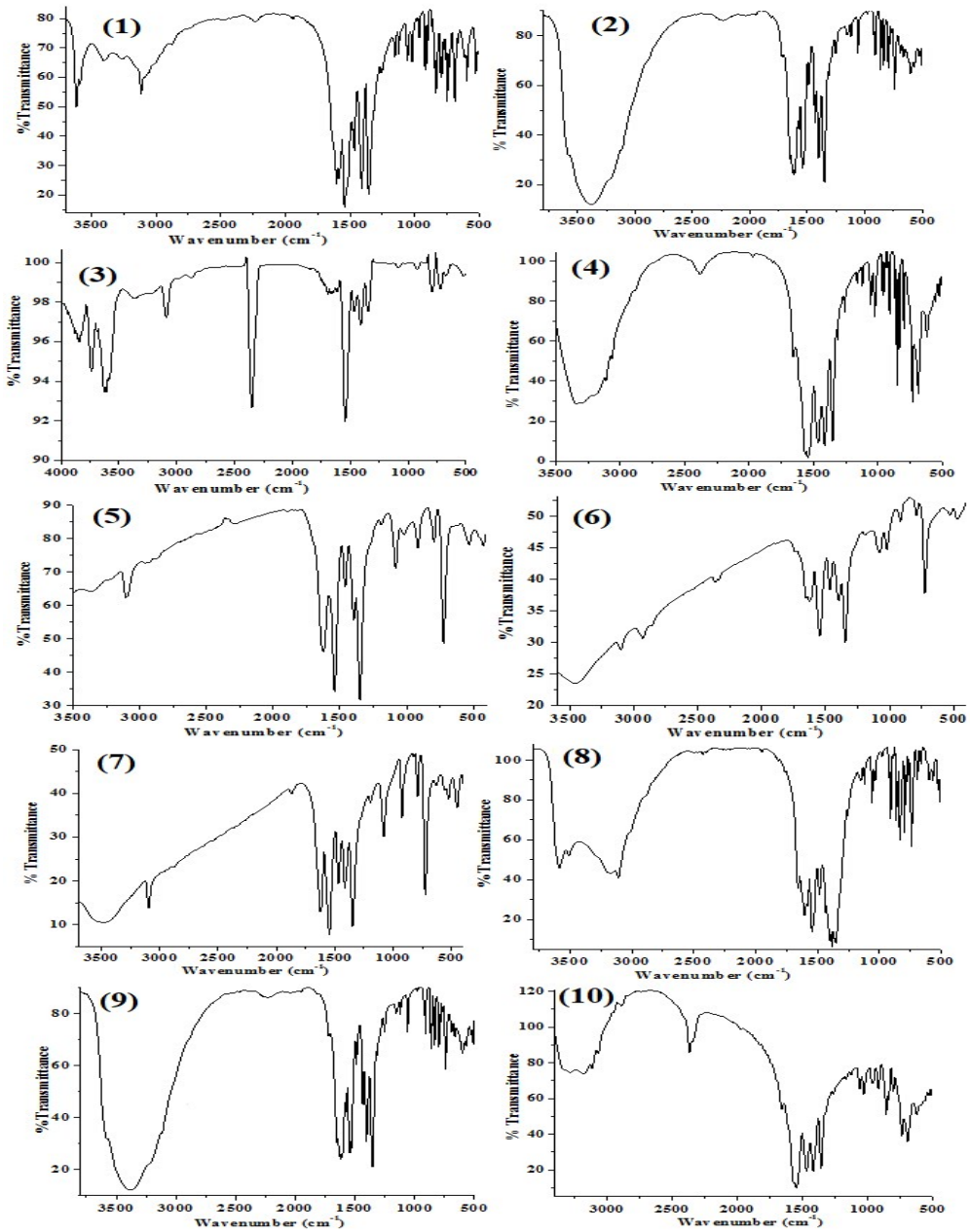

Figure S16. IR spectra of complexes **1-10**.

Powder X-ray Diffraction studies

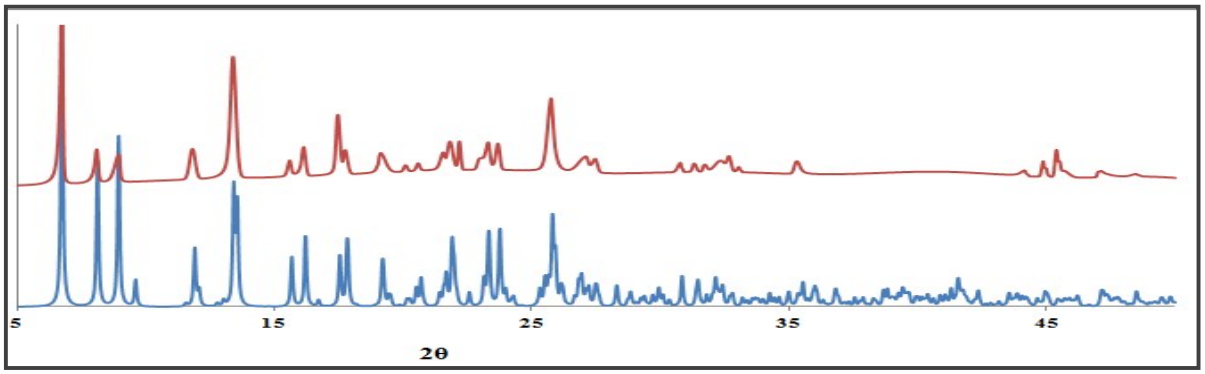

Fig S17. Showing generated (blue) and experimental (red) PXRD of complex (**1**)

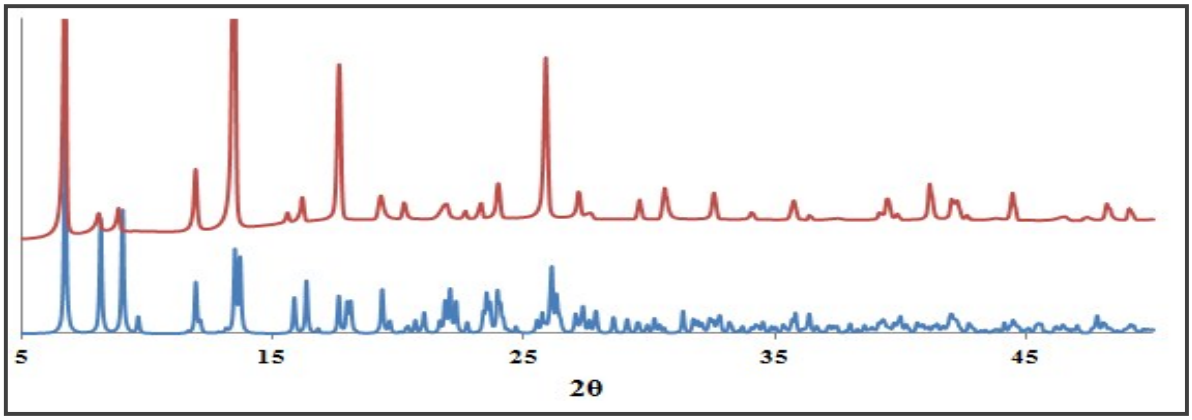

Fig S18. Showing generated (blue) and experimental (red) PXRD of complex (**2**)

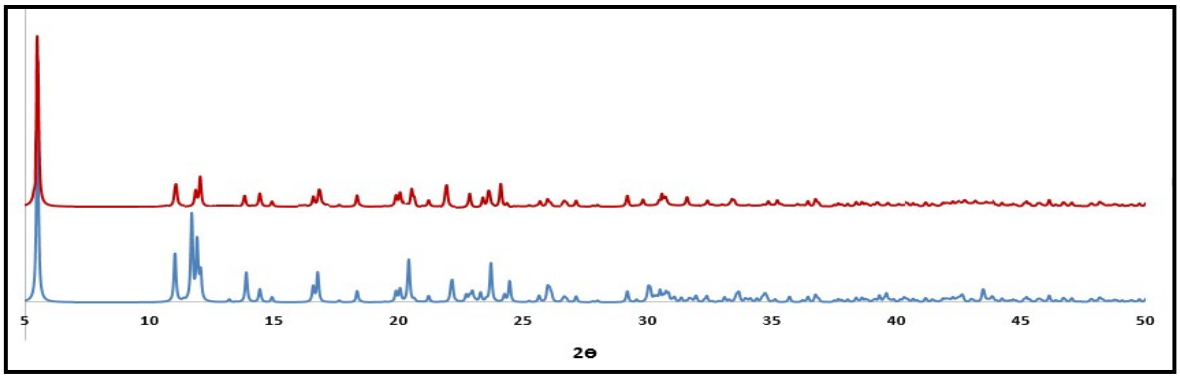

Fig S19. Showing generated (blue) and experimental (red) PXRD of complex (**3)**

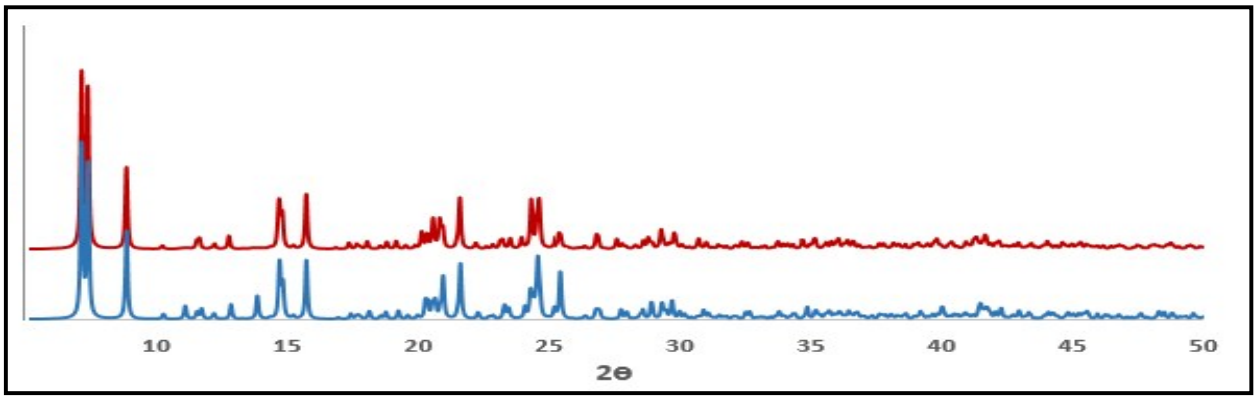

Fig S20. Showing generated (blue) and experimental (red) PXRD of complex (**4)**

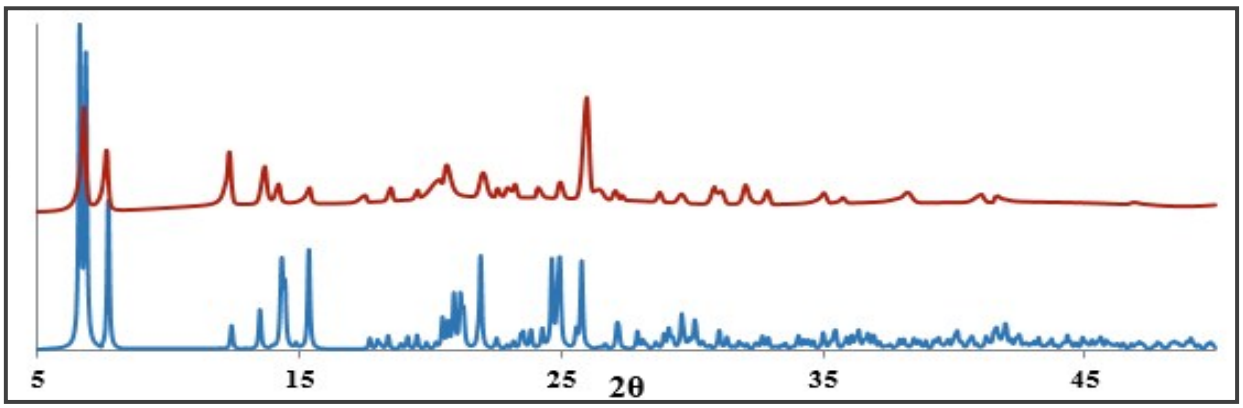

Fig S21. Showing generated (blue) and experimental (red) PXRD of complex (**5**)

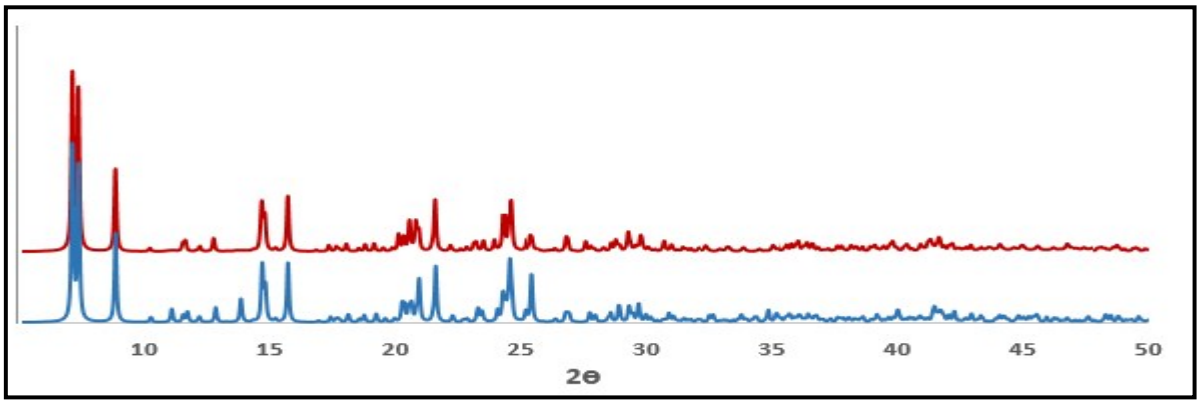

Fig S22. Showing generated (blue) and experimental (red) PXRD of complex (**6)**

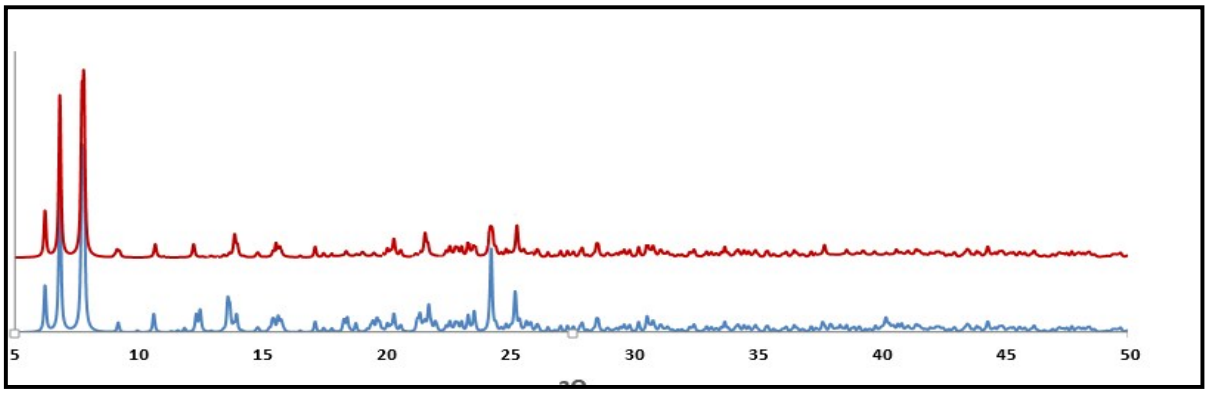

Fig S23. Showing generated (blue) and experimental (red) PXRD of complex (**7)**

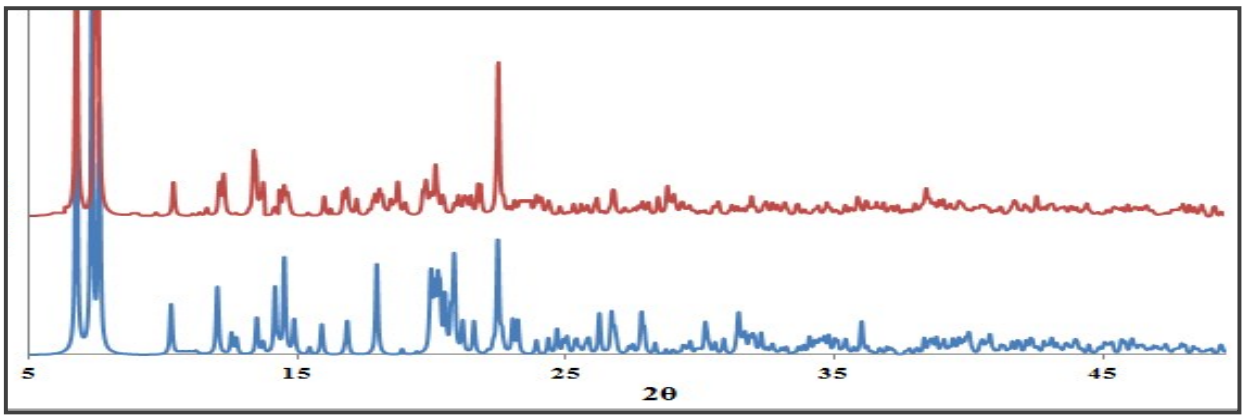

Fig S24. Showing generated (blue) and experimental (red) PXRD of complex (**8**)

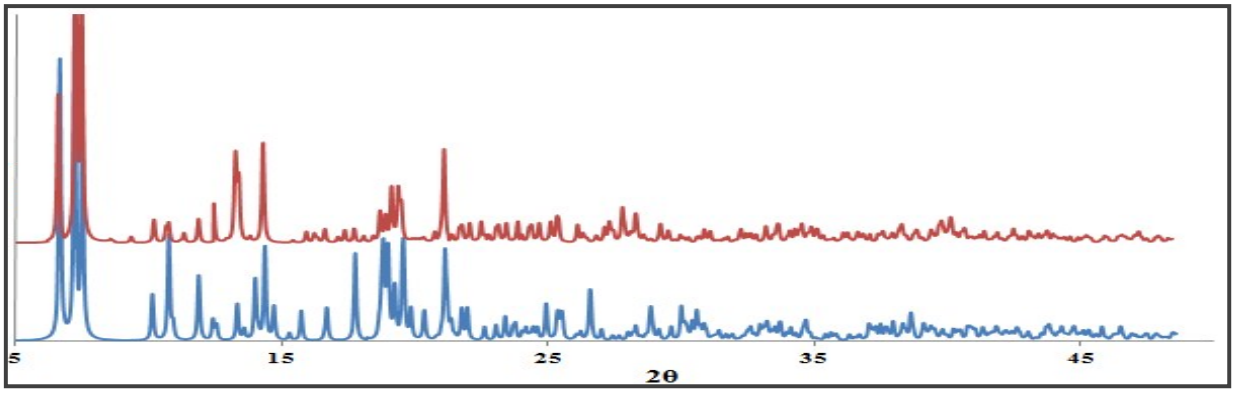

Fig S25. Showing generated (blue) and experimental (red) PXRD of complex (**9**)

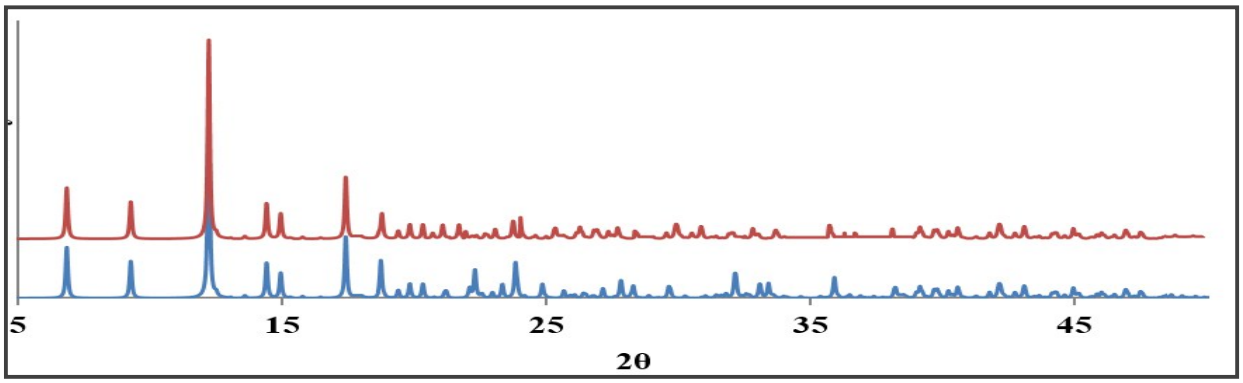

Fig S26. Showing generated (blue) and experimental (red) PXRD of complex (**10**)

Thermogravimetric analysis

The thermal stability of complexes **1-10** was examined by TGA (Fig. S13). Thermal decomposition curve of **1** shows that at 92 °C, a loss of 2.07 % (*calcd* 2.16 %) weight due to one lattice water molecule (*wt lost* 97.93 %, *calcd* 97.84 %). After that at 180 °C, a loss of two coordinated water molecules took place (*wt lost* 93.48 %, *calcd* 93.51 %). Two endothermic peaks (-1.62 and -0.98 W/g) are observed at 91 °C and at 179 °C, respectively due to a loss of lattice and coordinated water molecules. The complex is stable up to 420 °C and decomposition takes place in single step above that with one sharp exothermic peak (2.15 W/g) due to decomposition of parent complex with explosion. The TGA curve of **2** showed that at 92 °C, there is a loss of 2.07 % weight due to a loss of one lattice water molecule (*wt lost* 97.93 %, *calcd* 97.84 %). Then there is a loss of two coordinated water molecules up to 180 °C (*wt lost* 93.48 %, *calcd* 93.51 %). The complex is stable up to 420 °C and complete decomposition of parent complex took place in single step above that temperature with explosion. There are two endothermic peaks of -1.62 and -0.98 W/g are found at 91 °C and 179 °C, respectively due to a loss of lattice and coordinated water molecules. After that at 420 °C, there is a sharp exothermic peak of 2.15 W/g was observed due to complete decomposition with explosion. Complex **3** is stable up to 68 °C, after that it loses 5.44 % weight of two coordinated water molecules (*wt lost* 95.49 %, *calcd* 95.67 %) and at 215 °C, it loses 8.9 % weight due to one acetate anion (*wt lost* 84.34 %, *calcd* 84.37 %), beyond that it is stable up to 244 °C where it finally decomposes with explosion giving a sharp exothermic peak of 0.343 W/g. Thermal decomposition curve of **4** shows the loss of 4.62 % weight at 64 °C due to the removal of four lattice water molecules (*wt lost* 95.38 %, *calcd* 95.61 %). The complex is stable up to 306 °C and decomposition took place in single step above that temperature with 2.82 % weight is lost after complete decomposition of parent complex with explosion. There are

endothermic peaks of -0.05, 0.046 and 0.087 W/g observed at 64 ^{o}C, 174 ^{o}C and 236 ^{o}C, respectively. One sharp exothermic peak of 0.36 W/g is observed at 306 ^{o}C due to decomposition with explosion in complex **5**, there is a loss of four coordinated water molecules at 65 ^{o}C (*wt lost* 4.58 %, *calcd* 4.45 %). After that, a gradual weight loss is observed up to 298 ^{o}C resulting metal oxides as residue and a sharp weight loss with explosion. One endothermic peak of 0.165 W/g is observed at 62 ^{o}C due to a loss of lattice water molecules and small endothermic peaks of 0.25 W/g and 0.287 W/g are observed at 164 ^{o}C and 226 ^{o}C, respectively. A sharp exothermic peak of 0.548 W/g is observed at 307 ^{o}C due to an explosion of complete residue. In complex **6**, there is a loss of four coordinated water molecules in two steps up to 150 ^{o}C (*wt lost* 4.79 %, *calcd* 4.47 %). After that, the gradual weight loss is observed up to 400 ^{o}C and a sharp weight loss with explosion. Two endothermic peaks of -2.80W/g and -2.76W/g are observed at 115 ^{o}C and 191 ^{o}C, respectively due to a loss of coordinated water molecules. One exothermic peak of 0.67 W/g is observed at 400 ^{o}C due to explosion of complete residue. In complex **7**, there is a loss of 4.95 % weight due to coordinated solvent molecule DMF at 104 ^{o}C (*wt lost* 95.05 %, *calcd* 95.63 %). After that at 210 ^{o}C, there is a loss of three coordinated water molecules (*wt lost* 91.83 % *calcd*, 92.4 %). Then, a gradual weight loss is observed from 240 ^{o}C to 370 ^{o}C and then sharp decrease to 0 % weight at 400 ^{o}C. There are exothermic peaks of 12.89, 13.13 and 24.4 W/g observed at 120 ^{o}C, 240 ^{o}C and 400 ^{o}C, respectively. In complex **8**, there is a loss of six coordinated water molecules at 125 ^{o}C (*wt lost* 6.64 %, *calcd* 6.31 %). After that, gradual decomposition took place in two steps at 204 ^{o}C and 360 ^{o}C and then sharp decomposition at 361 ^{o}C is observed with 2.38 % weight lost as residue. The weak endothermic peaks of -0.048, 0.048 and 0.087 W/g are observed at 58 ^{o}C, 158 ^{o}C and 217 ^{o}C, respectively due to stepwise removal of coordinated water molecules. The sharp exothermic peak of 0.359 W/g is observed at 289 ^{o}C due to complete decomposition with explosion.

In case of complex **9**, there is removal of one coordinated water molecule at 44 ^{o}C (*wt lost* 2.70 %, *calcd* 2.68 %). After that, a removal of other two coordinated water molecules is observed at 123 ^{o}C (*wt lost* 5.37 %, *calcd* 5.32 %). From 210 ^{o}C to 414 ^{o}C, the decomposition of organic ligand is observed. After that at 435 ^{o}C, 41.7 % weight is lost as metal oxide. The endothermic peak at 228 ^{o}C is observed due to a removal of organic ligand and a sharp exothermic peak of 0.174W/g is observed at 341 ^{o}C due to complete decomposition of complex. Thermal decomposition curve of **10** shows the loss

of four coordinated water molecules at 108 °C (*wt lost* 6.69 %, *calcd* 6.89 %). After that, four acetate groups are decomposed up to 241 °C (*wt lost* 23.28 %, *calcd* 22.6 %). The complex starts decomposition after that and decomposition took place in single step. A sharp exothermic peak of 0.341 W/g is observed at 246 °C due to complete decomposition.

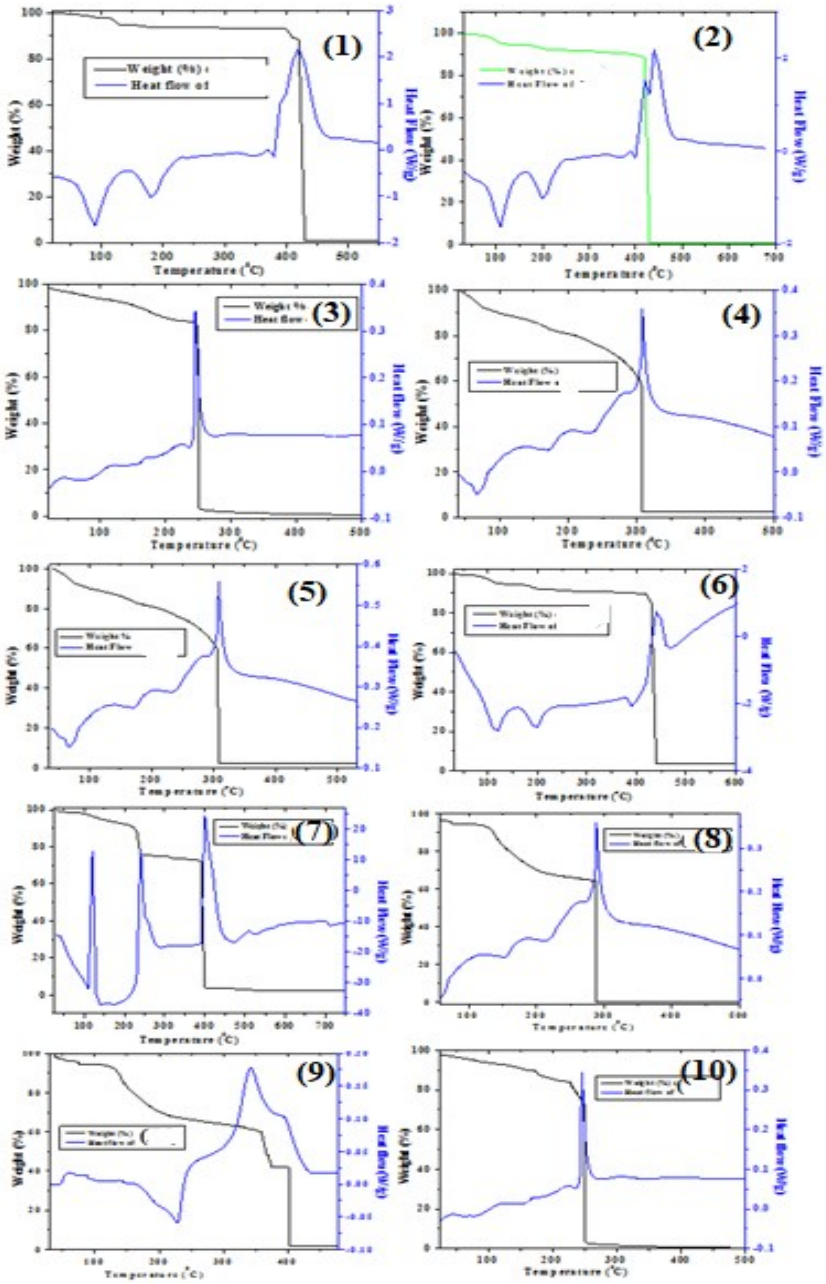

Figure S27. TGA plots of complexes **1-10**.

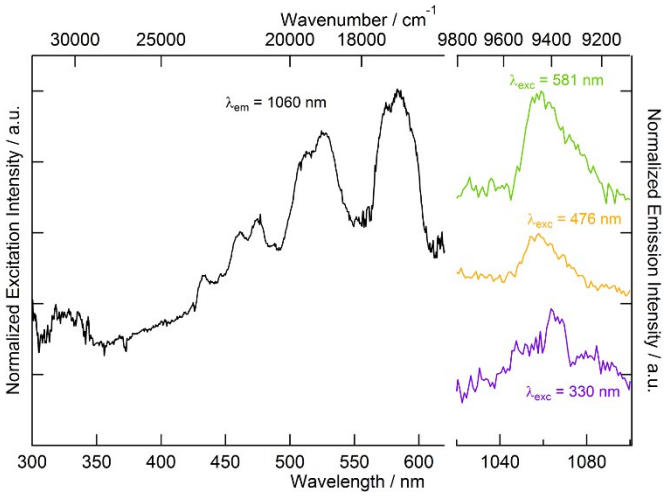

Figure S28. Solid-state excitation (black curve) and emission spectra of **3** at room temperature (λ_{ex} = 581 nm, green curve; λ_{ex} = 476 nm, yellow curve and λ_{ex} = 330 nm, purple curve). The intensities have been normalized on the more intense band at 581 nm and at 1060 nm for the excitation and emission spectra, respectively.

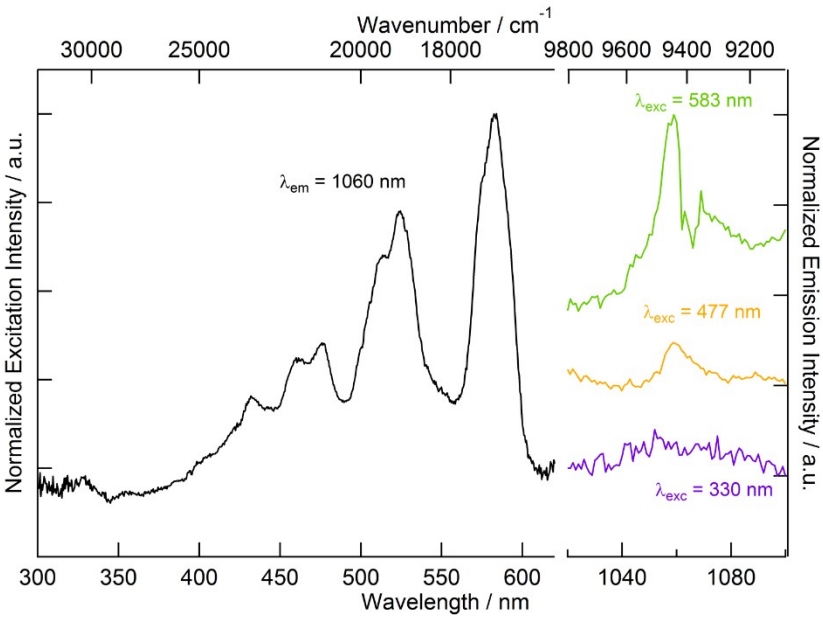

Figure S29. Solid-state excitation (black curve) and emission spectra ((λ_{ex} = 583 nm (green curve), λ_{ex} = 477 nm (yellow curve) and λ_{ex} = 330 nm (purple curve)) of **1** at room temperature. The intensities have been normalized on the more intense band at 583 nm and at 1060 nm for the excitation and emission spectra, respectively.

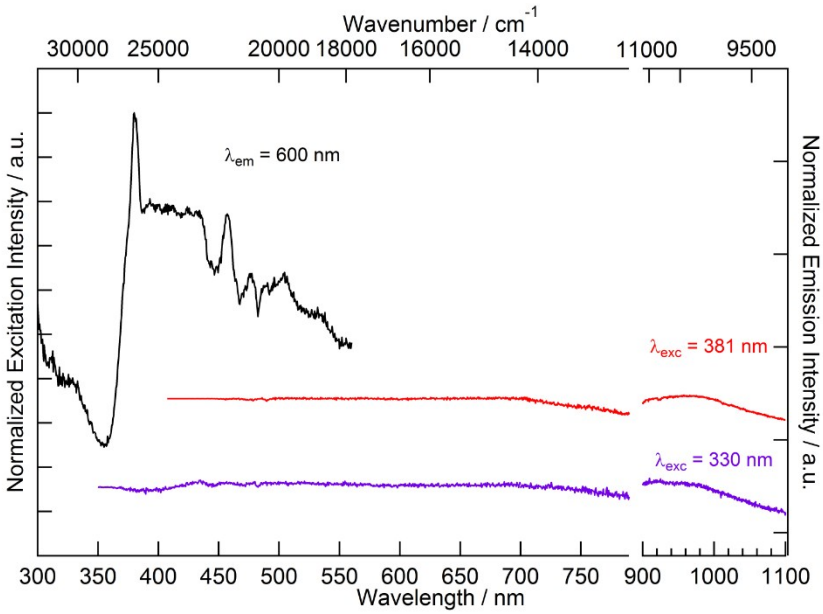

Figure S30. Solid-state excitation (black curve) and emission spectra ((λ_{ex} = 381 nm (red curve) and λ_{ex} = 330 nm (purple curve)) of **6** at room temperature. The intensity has been normalized on the more intense band for the green curve at 381 nm.

Dynamic magnetic measurements

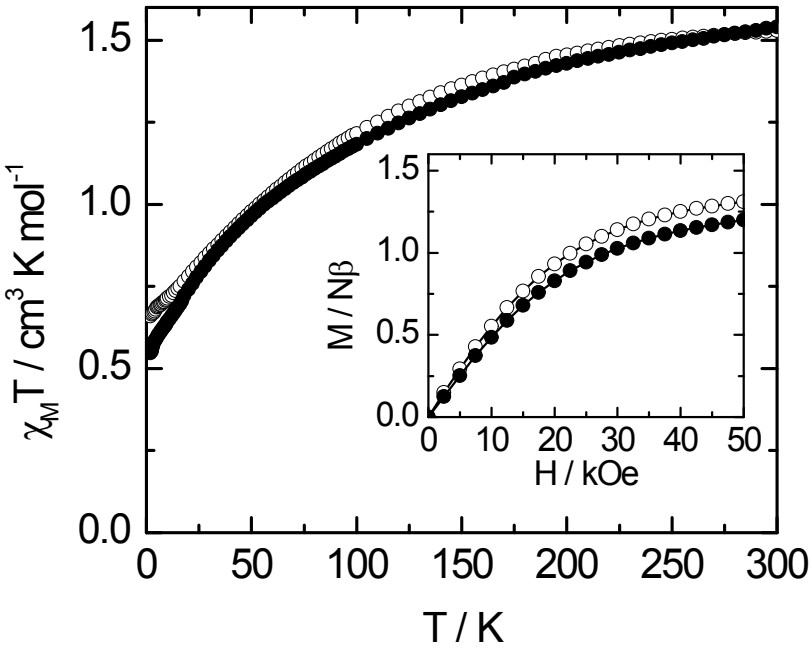

Figure S31. Temperature dependences of $\chi_M T$ for compounds **1** (black circles) and **3** (white circles). Inset: Magnetic field dependences of the magnetization for compounds **1** (black circles) and **3** (white circles) at 2 K.

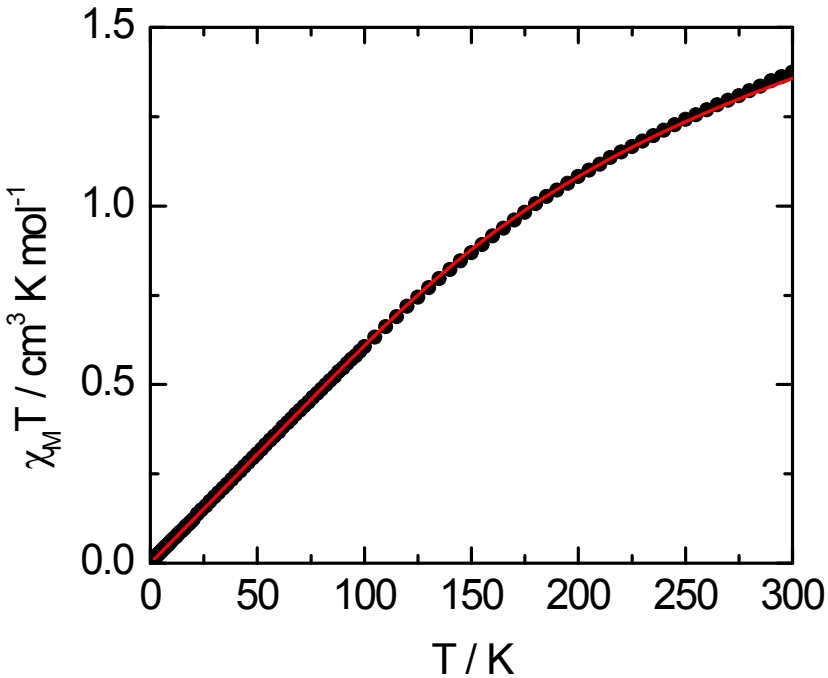

Figure S32. Temperature dependences of $\chi_M T$ for compound **2** (black circles) with the best fitted curve (red line) with the theoretical expression here below.

Magnetism of Eu^{III} complexes:

The spin-orbit coupling operator is:

$\hat{H} = \lambda \hat{\boldsymbol{L}} \cdot \hat{\boldsymbol{S}}$ where λ is the spin-orbit coupling parameter.

The energies of $\boldsymbol{J} = \boldsymbol{L} + \boldsymbol{S}$ states are:

$E(J) = \lambda J(J+1)/2$ where the energy of $^7F_0$ state has been taken as the origin.

The magnetic susceptibility considering that excited states (^7F_J with J = 1 to 5) can be thermally populated is expressed as

$$\chi_M = \frac{\sum_{J=0}^{6}(2J+1)\chi_M(J)\exp\left[\frac{-\lambda J(J+1)}{2kT}\right]}{\sum_{J=0}^{6}(2J+1)\exp\left[\frac{-\lambda J(J+1)}{2kT}\right]}$$

With $\chi_M(J) = \frac{Ng_J^2\beta^2 J(J+1)}{3kT} + \frac{2N\beta^2(g_J-1)(g_J-2)}{3\lambda}$ and

$$g_J = \frac{3}{2} + \frac{S(S+1) - L(L+1)}{2J(J+1)}$$

The first term is the Curie law and the second term is the temperature Independent Paramagnetism (TIP) which is due to the field induced mixing with close excited states. In this frame χ_M can be rewritten:

$$\chi_M = \frac{N\beta^2}{3kTx}\frac{\left[\begin{array}{c}24 + \left(\frac{27x}{2} - \frac{3}{2}\right)e^{-x} + \left(\frac{135x}{2} - \frac{5}{2}\right)e^{-3x} + \left(189x - \frac{7}{2}\right)e^{-6x} + \left(405x - \frac{9}{2}\right)e^{-10x} \\ + \left(\frac{1485x}{2} - \frac{11}{2}\right)e^{-15x} + \left(\frac{2457x}{2} - \frac{13}{2}\right)e^{-21x}\end{array}\right]}{1 + 3e^{-x} + 5e^{-3x} + 7e^{-6x} + 9e^{-10x} + 11e^{-15x} + 13e^{-21x}}$$

with $x = \frac{\lambda}{kT}$

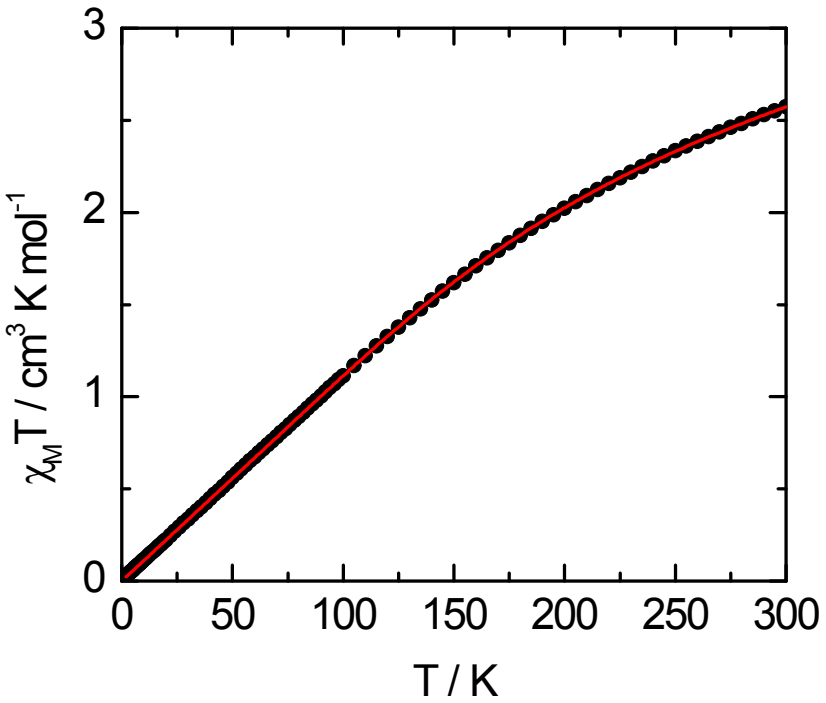

Figure S33. Temperature dependences of $\chi_M T$ for compound **8** (black circles) with the best fitted curve (red line) with the theoretical expression here above adapted for two Eu^{III} per chemical unit.

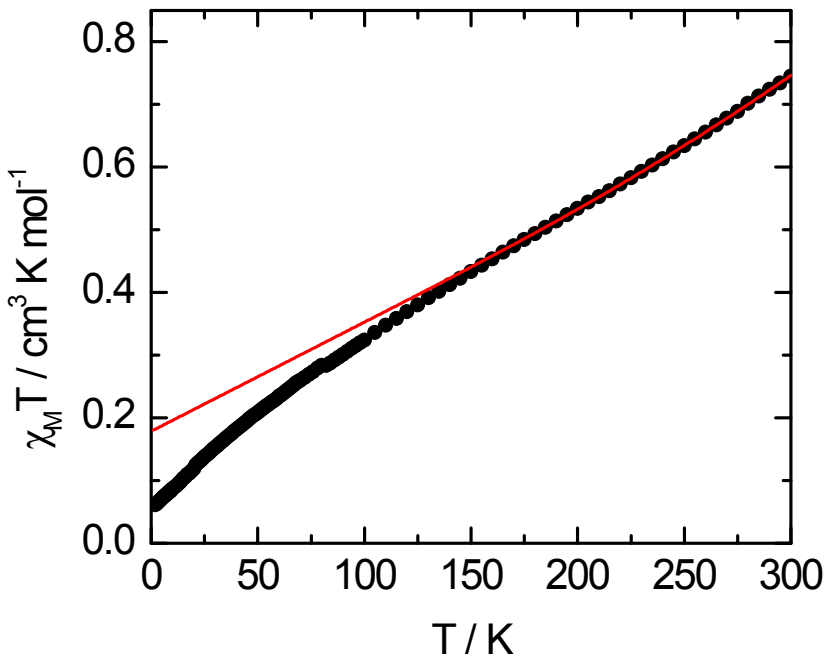

Figure S34. Temperature dependences of $\chi_M T$ for compound **4** (black circles) with the best fitted curve with the theoretical expression here below.

Magnetism of Sm^{III} complexes:

The thermal behaviour of the molar magnetic susceptibility for Sm^{III} complexes can be easily derived with the same methodology than for Eu^{III} complexes with

$E(J)=\frac{\lambda}{2}\left(J\left(J+1\right)-\frac{35}{4}\right)$ with the multiplet ground state $^6H_{5/2}$ taken as the origin.

The magnetic susceptibility considering that excited states (^6H_J with J = 7/2 to 15/2) can be thermally populated is expressed as

$$\chi_M=\frac{\sum_{J=5/2}^{15/2}\left(2J+1\right)\chi_M\left(J\right)\exp\left[-\frac{E\left(J\right)}{kT}\right]}{\sum_{J=5/2}^{15/2}\left(2J+1\right)\exp\left[-\frac{E\left(J\right)}{kT}\right]}$$

With $\chi_M\left(J\right)=\frac{Ng_J^2\beta^2J\left(J+1\right)}{3kT}+\frac{2N\beta^2\left(g_J-1\right)\left(g_J-2\right)}{3\lambda}$

In this frame χ_M (for one Sm^{III} site) can be rewritten:

$$\chi_M=\frac{N\beta^2}{3kT}\frac{\left[\begin{array}{c}6\left(\frac{5}{7}+\frac{120}{49x}\right)+8\left(\frac{2028}{2189}+\frac{4884}{11907x}\right)e^{-\frac{7x}{2}}+10\left(\frac{8427}{2297}-\frac{3864}{29403x}\right)e^{-8x}\\+12\left(\frac{22188}{429}-\frac{6612}{20449x}\right)e^{-\frac{27x}{2}}+14\left(\frac{9375}{117}-\frac{1848}{4563x}\right)e^{-20x}\\+16\left(\frac{1020}{9}-\frac{12}{27x}\right)e^{-\frac{55x}{2}}\end{array}\right]}{6+8e^{-\frac{7x}{2}}+10e^{-8x}+12e^{-\frac{27x}{2}}+149e^{-20x}+16e^{-\frac{55x}{2}}}$$ [i]

[i] *The expression given in the book of O. Kahn (Molecular Magnetism, VCH: Weinhem, **1993**) is erroneous.*

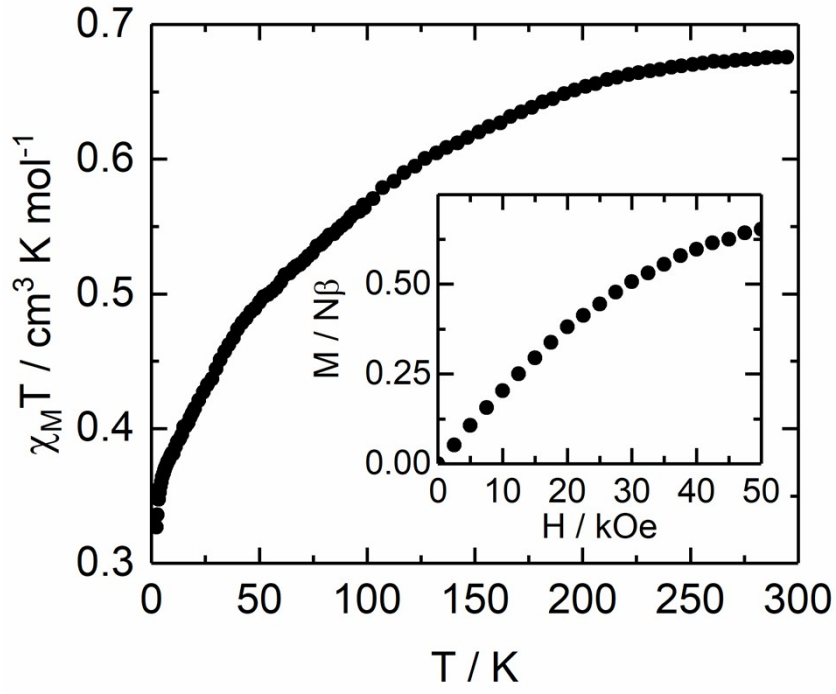

Figure S35. Temperature dependences of $\chi_M T$ for compound **5**. In inset, the field variation of the magnetization at 2 K.

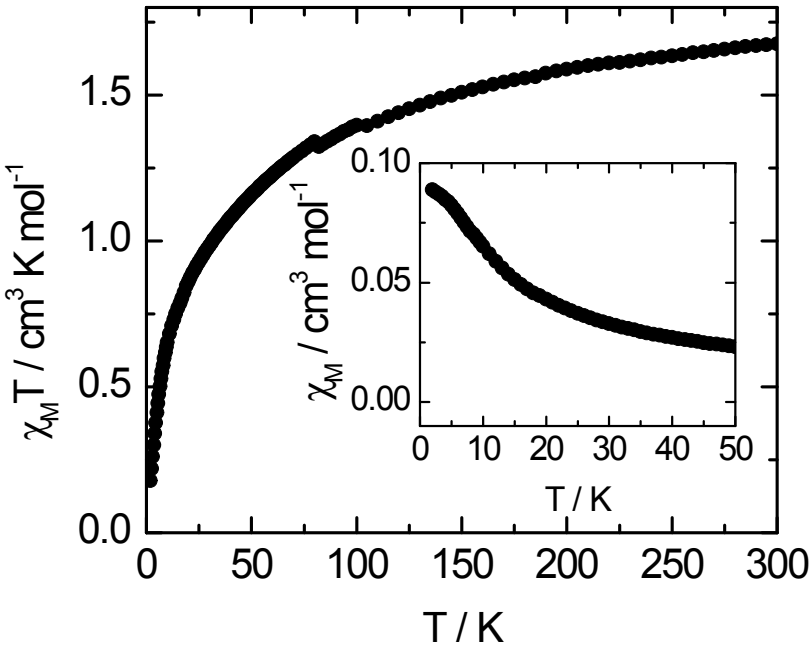

Figure S36. Temperature dependences of $\chi_M T$ for compound **6**. In inset the χ_M vs. T curve at low temperature.

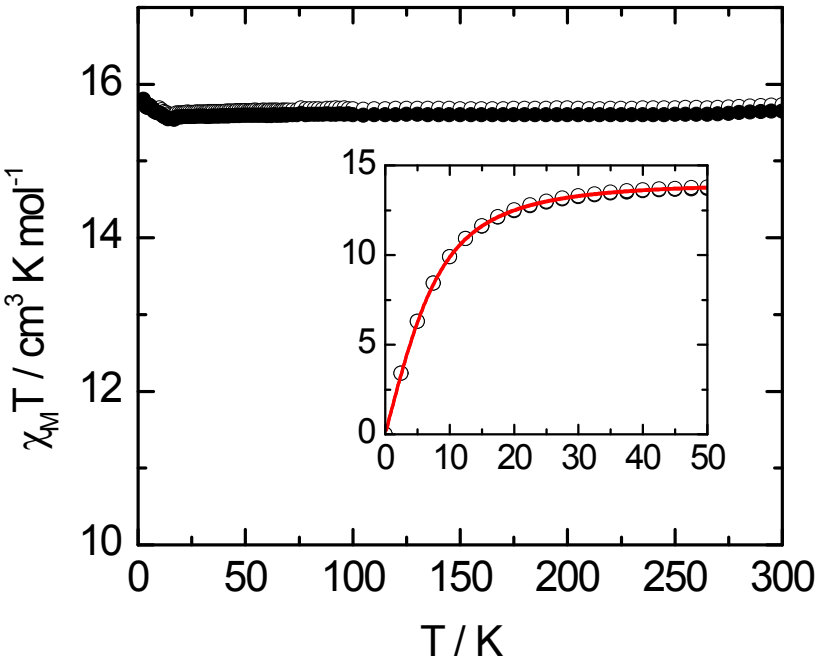

Figure S37. Temperature dependences of $\chi_M T$ for compounds **9** (white circles) and **10** (black circles). In inset the field variation of the magnetization at 2 K for the same two compounds with the best fitted curves (red lines) with a Brillouin function for two spins S=7/2.

X-ray crystallography

Table S1. Crystallographic Data for compounds **1-10**.

Identification code	**1**	**2**	**3**	**4**	**5**
Empirical formula	$C_{21}H_{15}N_6NdO_{21}$	$C_{21}H_{15}N_6O_{21}Eu$	$C_{16}H_{13}N_4NdO_{16}$	$C_{42}H_{18}N_{12}O_{40}Sm_2$	$C_{42}H_{24}N_{12}O_{40}Ce_2$
Formula weight	831.63	839.35	661.54	1631.41	1616.97
Temperature	296(2) K	100(2) K	296(2) K	296(2) K	296(2) K
Wavelength	0.71073 Å	0.71073 Å	0.71073 Å	0.71073 Å	0.71073 Å
Crystal system	Triclinic	Triclinic	Triclinic	Monoclinic	Monoclinic
Space group	$P\bar{1}$	$P\bar{1}$	$P\bar{1}$	Cc	Cc
Unit cell dimensions	a = 9.2950(6) Å, α = 106.487(3)°	a = 9.2090(17) Å, α = 106.024(8)°	a = 8.9260(9) Å, α = 75.642(3)°	a = 12.8390(14) Å, α = 90°	a = 12.7786(18) Å, α = 90°
	b = 11.472(8) Å, β = 90.356(3)°	b = 11.329(2) Å, β = 90.136(9)°	b = 8.983(8) Å, β = 77.479(3)°	b = 47.454(6) Å, β = 92.811(4)°	b = 47.775(7) Å, β = 92.972(5)°
	c = 13.821(10) Å, γ = 94.15(3)°	c = 13.664(3) Å, γ = 94.491(9)°	c = 16.6560(16) Å, γ = 61.240(3)°	c = 9.2030(9) Å, γ = 90°	c = 9.2651(10) Å, γ = 90°
Volume	1408.91(17) Å^3	1365.5(5) Å^3	1126.70(19) Å^3	5600.3(11) Å^3	5648.8(13) Å^3
Z	2	2	2	4	4
Density (calculated)	1.960 Mg/m^3	2.041 Mg/m^3	1.950 Mg/m^3	1.935 Mg/m^3	1.901 Mg/m^3
Absorption coefficient	1.952 mm^{-1}	2.409 mm^{-1}	2.395 mm^{-1}	2.202 mm^{-1}	1.716 mm^{-1}
F(000)	822	828	650	3192	3184
Crystal size	0.22 x 0.18 x 0.17 mm^3	0.16 x 0.13 x 0.10 mm^3	0.24 x 0.21 x 0.18 mm^3	0.18 x 0.17 x 0.15 mm^3	0.24 x 0.22 x 0.19 mm^3
Theta range for data collection	1.54 to 30.88°.	1.55 to 31.81°.	2.54 to 32.61°.	1.64 to 27.97°.	1.65 to 27.79°.
Index ranges	-13<=h<=13, -15<=k<=16,	-13<=h<=12, -16<=k<=16,	-13<=h<=13, -13<=k<=13,	-14<=h<=16, -60<=k<=62,	-16<=h<=16, -55<=k<=62,
	-19<=l<=19	-19<=l<=20	-25<=l<=25	-7<=l<=12	-8<=l<=12
Reflections collected	30525	28187	30227	26340	25602
Independent reflections	8562 [R(int) = 0.0491]	8849 [R(int) = 0.1450]	8090 [R(int) = 0.0365]	10017 [R(int) = 0.0798]	11222 [R(int) = 0.0688]
Completeness to theta = 25.242°	98.0 %	98.9 %	99.5 %	100 %	99.6 %
Absorption correction	Semi-empirical from equivalents	Semi-empirical from equivalents	Semi-empirical from equivalents	Semi-empirical from equivalents	Semi-empirical from equivalents
Max. and min. transmission	0.738 and 0.668	0.799 and 0.692	0.677 and 0.592	0.741 and 0.690	0.742 and 0.681
Refinement method	Full-matrix least-squares on F^2	Full-matrix least-squares on F^2	Full-matrix least-squares on F^2	Full-matrix least-squares on F^2	Full-matrix least-squares on F^2
Data / restraints / parameters	8562 / 6 / 460	8849 / 6 / 460	8090 / 4 / 346	10017 / 2 / 885	11222 / 11 / 883
Goodness-of-fit on F^2	0.954	1.084	1.091	0.878	0.901
Final R indices [I>2sigma(I)]	R1 = 0.0406, wR2 = 0.0784	R1 = 0.0685, wR2 = 0.1649	R1 = 0.0318, wR2 = 0.0788	R1 = 0.0522, wR2 = 0.1174	R1 = 0.0541, wR2 = 0.1280
R indices (all data)	R1 = 0.0573, wR2 = 0.0851	R1 = 0.1269, wR2 = 0.2518	R1 = 0.0394, wR2 = 0.0855	R1 = 0.0759, wR2 = 0.1343	R1 = 0.0723, wR2 = 0.1451
Largest diff. peak and hole	1.225 and -1.142 e.Å^{-3}	4.489 and -6.413 e.Å^{-3}	2.594 and -0.930 e.Å^{-3}	2.284 and -1.224 e.Å^{-3}	1.556 and -2.144 e.Å^{-3}
CCDC No.	1584550	1584545	1584549	1584552	1584543

Identification code	**6**	**7**	**8**	**9**	**10**
Empirical formula	$C_{42}H_{18}N_{12}O_{40}Pr_2$	$C_{45}H_{31}N_{13}O_{40}La_2$	$C_{42}H_{30}N_{12}O_{42}Eu_2$	$C_{42}H_{30}N_{12}O_{42}Gd_2$	$C_{22}H_{26}N_4O_{24}Gd_2$
Formula weight	1612.51	1671.65	1678.70	1689.24	1044.95
Temperature	296(2) K	296(2) K	296(2) K	296(2) K	100(2) K
Wavelength	0.71073 Å	0.71073 Å	0.71073 Å	0.71073 Å	0.71073 Å
Crystal system	Monoclinic	Triclinic	Triclinic	Triclinic	Orthorhombic
Space group	*Cc*	$P\bar{1}$	$P\bar{1}$	$P\bar{1}$	*Pbca*
Unit cell dimensions	a = 12.771(3) Å, α = 90°.	a = 8.9791(13) Å, α = 81.559(8)°.	a = 8.893(3) Å, α = 63.296(11)°	a = 8.9350(7) Å, α = 63.305(3)°.	a = 14.1321(4) Å, α = 90°.
	b = 47.712(9) Å, β = 92.452(11)°	b = 14.499(2) Å, β = 89.492(7)°.	b = 13.631(4) Å, β= 79.353(13)°	b = 13.6750(12) Å, β = 79.447(4)°	b = 8.8970(3) Å, β = 90°.
	c = 9.221(2) Å, γ= 90°.	c = 23.157(4) Å, γ= 81.411(7)°.	c = 14.316(4) Å, γ= 72.448(11)°	c = 14.3180(13) Å, γ= 72.332(3)°	c = 25.7568(7) Å, γ= 90°.
Volume	5614(2) $Å^3$	2948.5(8) $Å^3$	1475.7(8) $Å^3$	1487.0(2) $Å^3$	3238.49(17) $Å^3$
Z	4	2	1	1	4
Density (calculated)	1.908 Mg/m^3	1.883 Mg/m^3	1.889 Mg/m^3	1.886 Mg/m^3	2.143 Mg/m^3
Absorption coefficient	1.841 mm^{-1}	1.553 mm^{-1}	2.230 mm^{-1}	2.334 mm^{-1}	4.166 mm^{-1}
F(000)	3168	1652	828	830	2024
Crystal size	0.16 x 0.14 x 0.12 mm^3	0.19 x 0.17 x 0.16 mm^3	0.19 x 0.16 x 0.12 mm^3	0.18 x 0.15 x 0.12 mm^3	0.17 x 0.15 x 0.13 mm^3
Theta range for data collection	1.65 to 27.26°.	1.57 to 30.25°.	1.59 to 33.22°.	1.59 to 28.04°.	1.58 to 35.44°.
Index ranges	-16<=h<=12, -54<=k<=60,	-12<=h<=12, -20<=k<=20,	-8<=h<=13, -20<=k<=20,	-11<=h<=11, -18<=k<=16,	-17<=h<=22, -8<=k<=14,
	-11<=l<=11	-32<=l<=32	-20<=l<=21	-18<=l<=18	-41<=l<=33
Reflections collected	24423	68102	25104	26132	30138
Independent reflections	9624 [R(int) = 0.0547]	17467 [R(int) = 0.0530]	9806 [R(int) = 0.0330]	7111 [R(int) = 0.0213]	7216 [R(int) = 0.0249]
Completeness to theta = 25.242°	100 %	100 %	93.5 %	100 %	99.9 %
Absorption correction	Semi-empirical from equivalents	Semi-empirical from equivalents	Semi-empirical from equivalents	Semi-empirical from equivalents	Semi-empirical from equivalents
Max. and min. transmission	0.814 and 0.751	0.795 and 0.751	0.781 and 0.672	0.772 and 0.671	0.619 and 0. 531
Refinement method	Full-matrix least-squares on F^2	Full-matrix least-squares on F^2	Full-matrix least-squares on F^2	Full-matrix least-squares on F^2	Full-matrix least-squares on F^2
Data / restraints / parameters	9624 / 2 / 865	17467 / 9 / 921	9806 / 6 / 470	7111 / 9 / 470	7216 / 4 / 249
Goodness-of-fit on F^2	0.973	1.001	1.077	0.971	1.279
Final R indices [I>2sigma(I)]	R1 = 0.0390, wR2 = 0.0732	R1 = 0.0381, wR2 = 0.0810	R1 = 0.0473, wR2 = 0.0972	R1 = 0.0176, wR2 = 0.0439	R1 = 0.0270, wR2 = 0.0603
R indices (all data)	R1 = 0.0532, wR2 = 0.0786	R1 = 0.0595, wR2 = 0.0902	R1 = 0.0729, wR2 = 0.1279	R1 = 0.0190, wR2 = 0.0449	R1 = 0.0325, wR2 = 0.0626
Largest diff. peak and hole	1.235 and -1.041 $e.Å^{-3}$	1.075 and -0.739 $e.Å^{-3}$	4.066 and -4.056 $e.Å^{-3}$	0.630 and -0.511 $e.Å^{-3}$	2.483 and -1.556 $e.Å^{-3}$
CCDC No.	1584551	1584548	1584544	1584547	1584546

Table S2. Possible important hydrogen bonding interactions for complexes **1-10**.

Complex **1**

X-H···Y	X···Y	H···Y	∠X-H···Y
O1W-H11W···O15	3.647(7)	2.84	166
O2W-H21W···O1	2.810(3)	2.50	103
O2W-H22W···O1W	2.766(5)	2.01	158
O3W-H31W···O1W[1]	3.242(5)	2.77	118
O3W-H32W···O1W[1]	3.242 (5)	2.94	105
O3W-H32W···O2W[1]	2.790 (3)	2.00	170
O3W-H32W···O8[1]	3.186 (3)	2.78	114
O1W-H12W···N6[2]	3.622(6)	2.93	143
O1W-H12W...O17[2]	3.156(6)	2.44	148
O1W-H12W...O18[2]	3.307(7)	2.74	128
O1W-H12W...O16[3]	3.253(7)	2.86	112
O2W-H21W...O5[4]	2.993(4)	2.25	151
O3W-H31W...O3[5]	3.167(4)	2.64	124
O3W-H31W...O4[5]	3.112(4)	2.39	148
O3W-H31W...N1[5]	3.308 (4)	2.69	133

(1) -x+1, -y, -z+1 (2) -x, -y, -z (3) -x+1, -y, -z (4) -x, -y+1, -z+1 (5) x, +y-1, +z

Complex **2**

X-H···Y	X···Y	H···Y	∠X-H···Y
O2W-H22W···O1	2.790(9)	2.50	101
O3W-H31W···O5	3.263(14)	2.72	126
O3W-H31W···O6	3.571(11)	2.91	138
O3W-H31W···O16[1]	3.168(15)	2.43	152
O1W-H12W···O4[2]	3.569(10)	2.99	130
O1W-H12W···O8[3]	3.143(10)	2.65	120
O1W-H12W···O2W[3]	2.775(9)	2.15	132
O2W-H22W···O3[4]	2.936 (12)	2.17	154
O3W-H32W···O18[4]	3.340 (11)	2.73	132
O1W-H11W···O6[5]	3.049 (11)	2.50	123
O1W-H11W···N2[5]	3.250 (12)	2.79	117
O1W-H11W···O3W[5]	3.207 (11)	2.50	144
O1W-H11W···O5[5]	3.128(12)	2.64	119
O3W-H32W···O15[6]	3.636(14)	2.91	149
O2W-H21W···O3W[6]	2.722(11)	2.16	126

(1) x, +y-1, +z-1 (2) -x+2, -y+2, -z+2 (3) -x+1, -y+2, -z+2 (4) -x+2, -y+1, -z+2 (5) x, +y+1, +z
(6) -x+1, -y+1, -z+2

Complex **3**

X-H···Y	X···Y	H···Y	∠X-H···Y
O1W-H12W···O1	2.994(4)	2.65	108
O1W-H12W...O2	3.294(3)	2.68	134
O2W-H21W...O14[1]	2.668(4)	1.85	170
O1W-H12W...O1[2]	2.774(3)	2.13	136
O1W-H12W...O2[2]	2.864(3)	2.60	101
O1W-H12W...O2W[2]	3.375(3)	2.87	123
O1W-H11W...O2W[2]	3.375(3)	2.87	125
O1W-H11W...O1[2]	2.774(3)	2.11	144
O2W-H22W...N1[2]	3.510(4)	2.77	154
O2W-H22W...O3[2]	2.961(4)	2.25	147
O2W-H22W...O4[2]	3.684(5)	2.93	155

(1) -x+2, -y+2, -z (2) -x+1, -y+2, -z

Complex 5

X-H···Y	X···Y	H···Y	∠X-H···Y
O2W-H21W···O2	2.746(9)	1.98	154
O2W-H21W···O3	3.368(12)	2.83	124
O3W-H31W···N11	3.617(12)	2.97	137
O3W-H31W···O27	3.463(12)	2.79	140
O3W-H31W···O33	3.205(12)	2.49	147
O4W-H42W···O14	2.804(10)	2.51	102
O4W-H42W···O36[1]	3.182(12)	2.41	156
O3W-H31W···O29[2]	2.994(13)	2.56	115
O2W-H22W···O9[3]	3.077(11)	2.32	152
O2W-H22W···O10[3]	3.406(13)	2.91	121
O3W-H32W···O20[3]	2.941(10)	2.62	105
O3W-H32W···O1W[3]	2.944(10)	2.21	148
O4W-H41W···O1[3]	2.728(9)	2.03	145
O2W-H22W···N3[3]	3.440(12)	2.82	133
O4W-H42W···O21[3]	2.917(11)	2.39	123

(1) x+1, +y, +z (2) x-1/2, -y+1/2+1, +z+1/2 (3) x, +y, +z+1

Complex 7

X-H···Y	X···Y	H···Y	∠X-H···Y
O1W-H11W···O25	2.759(3)	2.45	104
O2W-H21W···O26	2.879(3)	2.59	103

O2W-H21W···O37	2.826(3)	2.04	166
O3W-H32W···O2	2.836(4)	2.52	104
O3W-H32W···O3	3.036 (3)	2.22	171
O2W-H22W···O21[1]	3.078 (4)	2.73	109
O2W-H22W···O31[1]	2.868(4)	2.55	105
O2W-H22W···O33[1]	3.158(4)	2.36	173
O1W-H12W···O6[2]	3.339(4)	2.67	142
O1W-H12W···N2[2]	3.500(4)	2.71	166
O1W-H12W···O5[2]	2.884(4)	2.10	164
O1W-H11W···N12[3]	3.537(4)	2.86	143
O1W-H11W···O35[3]	3.033(4)	2.24	166
O1W-H11W···O36[3]	3.289(4)	2.82	119
O3W-H31W···O1W[4]	2.734(3)	1.94	163

(1) x+1, +y, +z (2) -x+1, -y+1, -z+2 (3) x+1, +y-1, +z (4) x-1, +y, +z

Complex 8

X-H···Y	**X···Y**	**H···Y**	**∠X-H···Y**
O1W-H12W···O13	2.623(8)	1.87	153
O2W-H22W···O4	3.303(6)	2.98	106
O1W-H11W···N1[1]	3.451(10)	2.75	145
O1W-H11W···O3[2]	2.978(9)	2.42	127
O2W-H21W···O7[2]	2.686(8)	1.87	174
O1W-H11W···O4[2]	3.194(10)	2.46	152
O1W-H11W···N1[2]	3.451(10)	2.75	147
O3W-H31W···O12[3]	3.329(13)	2.95	111
O3W-H32W···N4[3]	3.475(12)	2.81	139
O3W-H32W···O11[3]	2.898(10)	2.12	159
O3W-H32W···O12[3]	3.329(13)	2.88	116
O2W-H22W···O5[4]	3.489(10)	2.85	136
O2W-H22W···O6[4]	2.980(8)	2.17	173
O2W-H22W···N2[4]	3.575(9)	2.80	158
O3W-H31W···N2[4]	3.740(7)	2.96	160
O3W-H31W···O5[4]	2.865(6)	2.06	167

(1) -x+1, -y, -z+2 (2) x, +y, +z-1 (3) x, +y, +z+1 (4) -x+1, -y+1, -z+2

Complex 9

X-H···Y	**X···Y**	**H···Y**	**∠X-H···Y**
O1W-H12W···O4	3.298(2)	2.90	113
O2W-H22W···O7	2.830 (3)	2.56	101
O2W-H22W···O8	2.619(3)	1.86	158

O3W-H32W···O7	2.652 (2)	2.38	101
O3W-H31W···O18[1]	3.351(5)	2.99	110
O3W-H32W···N6[1]	3.496 (4)	2.98	125
O3W-H32W···O17[1]	2.903 (4)	2.26	138
O1W-H11W···O13[2]	2.696 (3)	1.89	173
O2W-H21W···N1[2]	3.464 (3)	2.75	150
O2W-H21W···O3[2]	2.994 (3)	2.41	131
O2W-H21W···O4[2]	3.199 (4)	2.46	154
O3W-H31W···O5[3]	2.868 (2)	2.06	170
O1W-H12W···N2[3]	3.587 (3)	2.80	165
O1W-H12W···O5[3]	3.497 (4)	2.84	140
O1W-H12W···O6[3]	2.997 (3)	2.20	171
O3W-H31W···N2[3]	3.752 (2)	2.99	157

(1) x, +y, +z-1 (2) -x+1, -y+2, -z+1 (3) -x+1, -y+1, -z+1

Complex 10

X-H···Y	**X···Y**	**H···Y**	**∠X-H···Y**
O1W-H12W···O8[1]	2.689 (2)	1.88	176
O2W-H21W···O10[1]	2.693(2)	1.897	169
O2W-H22W···O7[2]	2.696(2)	1.94	154
O1W-H11W···O2[3]	2.841(2)	2.03	172

(1) -x+1/2, +y+1/2, +z (2) x-1/2, +y-1, -z+1/2 (3) -x+1/2, -y, +z-1/2

Table S3. Important bond distances (Å) and bond angles (°) of complexes **1-10**.

Complex 1

O(1)-Nd(1)	2.478(2)
O(2W)-Nd(1)	2.579(2)
O(3W)-Nd(1)	2.513(2)
O(7)-Nd(1)	2.440(2)
O(8)-Nd(1)	2.392(2)
O(13)-Nd(1)	2.385(2)
O(14)-Nd(1)	2.470(2)
O(13)-Nd(1)-O(8)	143.06(8)
O(13)-Nd(1)-O(7)	75.45(8)
O(8)-Nd(1)-O(7)	101.28(7)
O(13)-Nd(1)-O(14)	128.84(7)
O(8)-Nd(1)-O(14)	77.16(7)
O(7)-Nd(1)-O(14)	140.09(8)
O(13)-Nd(1)-O(1)	81.55(8)
O(8)-Nd(1)-O(1)	77.76(8)

O(7)-Nd(1)-O(1)	139.04(8)
O(14)-Nd(1)-O(1)	80.31(8)
O(13)-Nd(1)-O(3W)	136.78(8)
O(8)-Nd(1)-O(3W)	72.65(8)
O(7)-Nd(1)-O(3W)	73.00(8)
O(14)-Nd(1)-O(3W)	68.51(8)
O(1)-Nd(1)-O(3W)	140.74(8)
O(13)-Nd(1)-O(2W)	72.18(8)
O(8)-Nd(1)-O(2W)	71.71(8)
O(7)-Nd(1)-O(2W)	73.38(8)
O(14)-Nd(1)-O(2W)	138.86(8)
O(1)-Nd(1)-O(2W)	67.46(8)
O(3W)-Nd(1)-O(2W)	124.00(8)

Complex 2

O(1)-Eu(1)	2.430(8)
O(2)-Eu(1)	2.948(5)
O(7)-Eu(1)	2.402(4)
O(8)-Eu(1)	2.352(7)
O(13)-Eu(1)	2.339(4)
O(14)-Eu(1)	2.430(4)
O(1W)-Eu(1)	2.456(2)
O(2W)-Eu(1)	2.530(1)
O(13)-Eu(1)-O(8)	142.7(2)
O(13)-Eu(1)-O(7)	76.2(2)
O(8)-Eu(1)-O(7)	101.4(1)
O(13)-Eu(1)-O(14)	128.7(1)
O(8)-Eu(1)-O(14)	76.6(2)
O(7)-Eu(1)-O(14)	140.3(2)
O(13)-Eu(1)-O(1)	81.0(2)
O(8)-Eu(1)-O(1)	77.7(2)
O(7)-Eu(1)-O(1)	139.6(2)
O(14)-Eu(1)-O(1)	79.5(2)
O(13)-Eu(1)-O(1W)	137.6(2)
O(8)-Eu(1)-O(1W)	72.7(2)
O(7)-Eu(1)-O(1W)	73.1(2)
O(14)-Eu(1)-O(1W)	68.5(2)
O(1)-Eu(1)-O(1W)	140.3(2)
O(13)-Eu(1)-O(2W)	72.4(2)
O(8)-Eu(1)-O(2W)	71.4(2)

O(7)-Eu(1)-O(2W)	73.1(2)
O(14)-Eu(1)-O(2W)	138.4(2)
O(1)-Eu(1)-O(2W)	68.4(2)
O(1W)-Eu(1)-O(2W)	123.6(2)
O(13)-Eu(1)-O(2)	66.1(2)
O(7)-Eu(1)-O(2)	140.0(2)
O(14)-Eu(1)-O(2)	65.9(2)
O(1)-Eu(1)-O(2)	47.22(1)
O(1W)-Eu(1)-O(2)	128.80(1)
O(2W)-Eu(1)-O(2)	105.9(2)
O(8)-Eu(1)-O(2)	116.3(2)

Complex 3

O(1)-Nd(1)	2.4404(18)
O(1W)-Nd(1)	2.536(2)
O(2W)-Nd(1)	2.488(2)
O(7)-Nd(1)	2.4837(19)
O(8)-Nd(1)	2.453(2)
O(13)-Nd(1)	2.5221(18)
O(14)-Nd(1)	2.5732(19)
O(1)-Nd(1)-O(8)	142.39(7)
O(1)-Nd(1)-O(7)	78.44(6)
O(8)-Nd(1)-O(7)	136.93(6)
O(1)-Nd(1)-O(2W)	71.97(7)
O(8)-Nd(1)-O(2W)	71.34(7)
O(7)-Nd(1)-O(2W)	138.03(7)
O(1)-Nd(1)-O(13)	124.76(6)
O(8)-Nd(1)-O(13)	72.38(7)
O(7)-Nd(1)-O(13)	70.17(6)
O(2W)-Nd(1)-O(13)	103.47(7)
O(1)-Nd(1)-O(1W)	73.95(7)
O(8)-Nd(1)-O(1W)	125.50(8)
O(7)-Nd(1)-O(1W)	66.79(7)
O(2W)-Nd(1)-O(1W)	128.82(8)
O(13)-Nd(1)-O(1W)	127.31(6)
O(1)-Nd(1)-O(14)	77.52(7)
O(8)-Nd(1)-O(14)	98.62(8)
O(7)-Nd(1)-O(14)	73.12(7)
O(2W)-Nd(1)-O(14)	71.93(7)
O(13)-Nd(1)-O(14)	50.68(6)

O(1W)-Nd(1)-O(14)	134.34(8)

Complex 4

O(1)-Sm(2)	2.513(10)
O(2)-Sm(2)	2.588(9)
O(1W)-Sm(1)	2.514(9)
O(2W)-Sm(2)	2.539(11)
O(3W)-Sm(1)	2.528(10)
O(4W)-Sm(1)	2.503(10)
O(7)-Sm(2)	2.391(9)
O(8)-Sm(1)	2.419(9)
O(13)-Sm(1)	2.347(9)
O(14)-Sm(2)	2.457(9)
O(19)-Sm(2)	2.388(10)
O(19)-Sm(1)	2.662(10)
O(20)-Sm(1)	2.481(11)
O(25)-Sm(1)	2.408(9)
O(25)-Sm(2)	2.658(9)
O(26)-Sm(2)	2.576(11)
O(31)-Sm(2)	2.341(9)
O(32)-Sm(1)	2.405(10)
O(13)-Sm(1)-O(32)	92.9(3)
O(13)-Sm(1)-O(25)	150.8(3)
O(32)-Sm(1)-O(25)	84.9(3)
O(13)-Sm(1)-O(8)	82.2(3)
O(32)-Sm(1)-O(8)	140.5(4)
O(25)-Sm(1)-O(8)	81.2(3)
O(13)-Sm(1)-O(20)	83.9(3)
O(32)-Sm(1)-O(20)	138.2(4)
O(25)-Sm(1)-O(20)	116.6(3)
O(8)-Sm(1)-O(20)	80.5(4)
O(13)-Sm(1)-O(4W)	73.3(3)
O(32)-Sm(1)-O(4W)	72.6(3)
O(25)-Sm(1)-O(4W)	78.3(3)
O(8)-Sm(1)-O(4W)	68.5(4)
O(20)-Sm(1)-O(4W)	143.3(4)
O(13)-Sm(1)-O(1W)	70.6(3)
O(32)-Sm(1)-O(1W)	73.2(3)
O(25)-Sm(1)-O(1W)	135.2(3)
O(8)-Sm(1)-O(1W)	138.6(3)

O(20)-Sm(1)-O(1W)	66.4(3)
O(4W)-Sm(1)-O(1W)	128.0(3)
O(13)-Sm(1)-O(3W)	134.9(3)
O(32)-Sm(1)-O(3W)	74.1(3)
O(25)-Sm(1)-O(3W)	72.4(3)
O(8)-Sm(1)-O(3W)	134.3(3)
O(20)-Sm(1)-O(3W)	79.0(3)
O(4W)-Sm(1)-O(3W)	137.0(3)
O(1W)-Sm(1)-O(3W)	64.3(3)
O(13)-Sm(1)-O(19)	128.3(3)
O(32)-Sm(1)-O(19)	136.0(3)
O(25)-Sm(1)-O(19)	66.5(3)
O(8)-Sm(1)-O(19)	69.5(3)
O(20)-Sm(1)-O(19)	50.2(3)
O(4W)-Sm(1)-O(19)	128.2(3)
O(1W)-Sm(1)-O(19)	103.5(3)
O(3W)-Sm(1)-O(19)	65.9(3)
O(13)-Sm(1)-C(36)	107.5(4)
O(32)-Sm(1)-C(36)	140.5(4)
O(25)-Sm(1)-C(36)	92.0(4)
O(8)-Sm(1)-C(36)	77.0(4)
O(20)-Sm(1)-C(36)	24.7(3)
O(4W)-Sm(1)-C(36)	145.1(4)
O(1W)-Sm(1)-C(36)	82.0(4)
O(3W)-Sm(1)-C(36)	67.5(4)
O(19)-Sm(1)-C(36)	25.9(3)
O(31)-Sm(2)-O(19)	147.0(3)
O(31)-Sm(2)-O(7)	139.9(3)
O(19)-Sm(2)-O(7)	72.8(3)
O(31)-Sm(2)-O(14)	108.3(3)
O(19)-Sm(2)-O(14)	81.7(3)
O(7)-Sm(2)-O(14)	74.0(3)
O(31)-Sm(2)-O(1)	73.6(4)
O(19)-Sm(2)-O(1)	79.5(3)
O(7)-Sm(2)-O(1)	140.2(3)
O(14)-Sm(2)-O(1)	74.2(3)
O(31)-Sm(2)-O(2W)	71.0(4)
O(19)-Sm(2)-O(2W)	141.8(3)
O(7)-Sm(2)-O(2W)	70.2(3)
O(14)-Sm(2)-O(2W)	79.3(4)

O(1)-Sm(2)-O(2W)	125.5(3)
O(31)-Sm(2)-O(26)	74.0(4)
O(19)-Sm(2)-O(26)	116.2(4)
O(7)-Sm(2)-O(26)	82.4(4)
O(14)-Sm(2)-O(26)	144.6(4)
O(1)-Sm(2)-O(26)	136.4(4)
O(2W)-Sm(2)-O(26)	68.0(4)
O(31)-Sm(2)-O(2)	74.4(3)
O(19)-Sm(2)-O(2)	73.8(3)
O(7)-Sm(2)-O(2)	139.7(3)
O(14)-Sm(2)-O(2)	122.4(3)
O(1)-Sm(2)-O(2)	50.8(3)
O(2W)-Sm(2)-O(2)	143.8(3)
O(26)-Sm(2)-O(2)	92.6(3)
O(31)-Sm(2)-O(25)	112.1(3)
O(19)-Sm(2)-O(25)	66.9(3)
O(7)-Sm(2)-O(25)	72.6(3)
O(14)-Sm(2)-O(25)	139.4(3)
O(1)-Sm(2)-O(25)	121.4(3)
O(2W)-Sm(2)-O(25)	109.7(3)
O(26)-Sm(2)-O(25)	49.7(3)
O(2)-Sm(2)-O(25)	73.9(3)

Complex 5

O(1)-Ce(1)	2.592(9)
O(2)-Ce(1)	2.646(8)
O(7)-Ce(1)	2.390(8)
O(8)-Ce(2)#1	2.459(9)
O(13)-Ce(1)	2.456(9)
O(13)-Ce(2)	2.698(9)
O(14)-Ce(2)	2.566(10)
O(19)-Ce(1)	2.530(8)
O(20)-Ce(2)#1	2.448(8)
O(25)-Ce(1)	2.457(8)
O(26)-Ce(2)	2.479(8)
O(31)-Ce(2)	2.489(8)
O(31)-Ce(1)	2.675(9)
O(32)-Ce(1)	2.663(11)
O(1W)-Ce(1)	2.632(8)

O(2W)-Ce(2)	2.572(9)
O(3W)-Ce(2)	2.524(10)
O(4W)-Ce(2)	2.555(8)
O(7)-Ce(1)-O(13)	147.4(3)
O(7)-Ce(1)-O(25)	140.1(3)
O(13)-Ce(1)-O(25)	71.9(3)
O(7)-Ce(1)-O(19)	111.7(3)
O(13)-Ce(1)-O(19)	79.4(3)
O(25)-Ce(1)-O(19)	72.8(3)
O(7)-Ce(1)-O(1)	74.6(3)
O(13)-Ce(1)-O(1)	79.3(3)
O(25)-Ce(1)-O(1)	140.1(3)
O(19)-Ce(1)-O(1)	75.3(3)
O(7)-Ce(1)-O(1W)	70.7(3)
O(13)-Ce(1)-O(1W)	141.9(3)
O(25)-Ce(1)-O(1W)	70.6(3)
O(19)-Ce(1)-O(1W)	83.9(3)
O(1)-Ce(1)-O(1W)	128.8(3)
O(7)-Ce(1)-O(2)	74.6(3)
O(13)-Ce(1)-O(2)	73.7(3)
O(25)-Ce(1)-O(2)	138.7(3)
O(19)-Ce(1)-O(2)	121.9(3)
O(1)-Ce(1)-O(2)	49.8(3)
O(1W)-Ce(1)-O(2)	142.8(3)
O(7)-Ce(1)-O(32)	74.3(3)
O(13)-Ce(1)-O(32)	114.8(3)
O(25)-Ce(1)-O(32)	81.4(3)
O(19)-Ce(1)-O(32)	145.1(4)
O(1)-Ce(1)-O(32)	136.7(3)
O(1W)-Ce(1)-O(32)	65.2(4)
O(2)-Ce(1)-O(32)	93.1(3)
O(7)-Ce(1)-O(31)	110.8(3)
O(13)-Ce(1)-O(31)	67.2(3)
O(25)-Ce(1)-O(31)	72.1(3)
O(19)-Ce(1)-O(31)	137.3(3)
O(1)-Ce(1)-O(31)	120.8(3)
O(1W)-Ce(1)-O(31)	106.3(3)
O(2)-Ce(1)-O(31)	74.1(3)
O(32)-Ce(1)-O(31)	48.1(3)
O(26)-Ce(2)-O(31)	80.7(2)

O(26)-Ce(2)-O(3W)	68.3(2)
O(31)-Ce(2)-O(3W)	79.0(2)
O(26)-Ce(2)-O(4W)	139.7(2)
O(31)-Ce(2)-O(4W)	134.1(2)
O(3W)-Ce(2)-O(4W)	128.5(2)
O(26)-Ce(2)-O(14)	81.0(3)
O(31)-Ce(2)-O(14)	115.8(2)
O(3W)-Ce(2)-O(14)	143.5(3)
O(4W)-Ce(2)-O(14)	66.4(2)
O(26)-Ce(2)-O(2W)	133.9(2)
O(31)-Ce(2)-O(2W)	72.0(2)
O(3W)-Ce(2)-O(2W)	137.3(2)
O(4W)-Ce(2)-O(2W)	63.4(2)
O(14)-Ce(2)-O(2W)	78.6(2)
O(26)-Ce(2)-O(13)	69.4(2)
O(31)-Ce(2)-O(13)	66.36(19)
O(3W)-Ce(2)-O(13)	128.5(2)
O(4W)-Ce(2)-O(13)	102.8(2)
O(14)-Ce(2)-O(13)	49.6(2)
O(2W)-Ce(2)-O(13)	65.9(3)

Complex 6

O(1)-Pr(1)	2.575(6)
O(2)-Pr(1)	2.642(5)
O(1W)-Pr(1)	2.581(6)
O(2W)-Pr(2)	2.571(6)
O(3W)-Pr(2)	2.557(5)
O(4W)-Pr(2)	2.526(6)
O(7)-Pr(1)	2.378(6)
O(8)-Pr(2)	2.438(6)
O(13)-Pr(1)	2.492(6)
O(14)-Pr(2)	2.424(6)
O(19)-Pr(1)	2.435(6)
O(20)-Pr(2)	2.455(5)
O(25)-Pr(2)	2.477(6)
O(25)-Pr(1)	2.662(6)
O(26)-Pr(1)	2.620(8)
O(31)-Pr(1)	2.441(6)
O(31)-Pr(2)	2.653(6)

O(32)-Pr(2)	2.532(7)
O(7)-Pr(1)-O(19)	140.1(2)
O(7)-Pr(1)-O(31)	147.03(19)
O(19)-Pr(1)-O(31)	72.06(19)
O(7)-Pr(1)-O(13)	111.5(2)
O(19)-Pr(1)-O(13)	73.5(2)
O(31)-Pr(1)-O(13)	80.19(19)
O(7)-Pr(1)-O(1)	74.3(2)
O(19)-Pr(1)-O(1)	140.5(2)
O(31)-Pr(1)-O(1)	79.7(2)
O(13)-Pr(1)-O(1)	75.0(2)
O(7)-Pr(1)-O(1W)	71.8(2)
O(19)-Pr(1)-O(1W)	70.0(2)
O(31)-Pr(1)-O(1W)	141.15(19)
O(13)-Pr(1)-O(1W)	81.4(2)
O(1)-Pr(1)-O(1W)	127.3(2)
O(7)-Pr(1)-O(26)	73.4(2)
O(19)-Pr(1)-O(26)	81.7(2)
O(31)-Pr(1)-O(26)	115.2(2)
O(13)-Pr(1)-O(26)	145.0(2)
O(1)-Pr(1)-O(26)	136.4(2)
O(1W)-Pr(1)-O(26)	67.0(2)
O(7)-Pr(1)-O(2)	73.87(18)
O(19)-Pr(1)-O(2)	139.25(18)
O(31)-Pr(1)-O(2)	73.88(17)
O(13)-Pr(1)-O(2)	121.6(2)
O(1)-Pr(1)-O(2)	49.53(18)
O(1W)-Pr(1)-O(2)	144.1(2)
O(26)-Pr(1)-O(2)	93.3(2)
O(7)-Pr(1)-O(25)	109.7(2)
O(19)-Pr(1)-O(25)	73.08(19)
O(31)-Pr(1)-O(25)	66.80(18)
O(13)-Pr(1)-O(25)	138.60(18)
O(1)-Pr(1)-O(25)	119.99(18)
O(1W)-Pr(1)-O(25)	108.9(2)
O(26)-Pr(1)-O(25)	49.00(19)
O(2)-Pr(1)-O(25)	73.38(18)
O(20)-Pr(2)-O(25)	81.3(2)
O(20)-Pr(2)-O(4W)	68.3(2)
O(25)-Pr(2)-O(4W)	78.89(19)

O(20)-Pr(2)-O(32)	80.4(2)
O(25)-Pr(2)-O(32)	116.2(2)
O(4W)-Pr(2)-O(32)	143.0(2)
O(20)-Pr(2)-O(3W)	139.0(2)
O(25)-Pr(2)-O(3W)	134.35(19)
O(4W)-Pr(2)-O(3W)	128.4(2)
O(32)-Pr(2)-O(3W)	66.5(2)
O(20)-Pr(2)-O(2W)	134.3(2)
O(25)-Pr(2)-O(2W)	71.37(19)
O(4W)-Pr(2)-O(2W)	136.4(2)
O(32)-Pr(2)-O(2W)	79.9(2)
O(3W)-Pr(2)-O(2W)	64.23(18)
O(20)-Pr(2)-O(31)	68.8(2)
O(25)-Pr(2)-O(31)	66.46(18)
O(4W)-Pr(2)-O(31)	127.79(18)
O(32)-Pr(2)-O(31)	49.90(18)
O(3W)-Pr(2)-O(31)	103.51(19)
O(2W)-Pr(2)-O(31)	66.87(18)

Complex 7

O(1)-La(1)	2.514(2)
O(2)-La(2)	2.573(2)
O(7)-La(1)	2.492(2)
O(7)-La(2)	2.865(2)
O(8)-La(2)	2.595(2)
O(13)-La(1)	2.805(2)
O(14)-La(1)	2.615(2)
O(19)-La(2)	2.640(2)
O(20)-La(2)	2.840(2)
O(25)-La(1)	2.602(2)
O(26)-La(2)	2.492(2)
O(26)-La(1)	2.881(2)
O(31)-La(1)#2	2.568(2)
O(32)-La(2)	2.478(2)
O(37)-La(2)	2.611(2)
O(1W)-La(1)	2.689(2)
O(2W)-La(1)	2.573(2)
O(3W)-La(2)	2.587(2)
O(7)-La(1)-O(1)	72.69(7)

O(7)-La(1)-O(2W)	77.19(8)
O(1)-La(1)-O(2W)	128.95(7)
O(7)-La(1)-O(25)	111.69(7)
O(1)-La(1)-O(25)	77.90(8)
O(2W)-La(1)-O(25)	76.28(8)
O(7)-La(1)-O(14)	80.66(7)
O(1)-La(1)-O(14)	71.15(7)
O(2W)-La(1)-O(14)	141.82(9)
O(25)-La(1)-O(14)	141.42(8)
O(7)-La(1)-O(1W)	138.08(7)
O(1)-La(1)-O(1W)	65.50(7)
O(2W)-La(1)-O(1W)	132.92(8)
O(25)-La(1)-O(1W)	62.83(7)
O(14)-La(1)-O(1W)	83.33(8)
O(7)-La(1)-O(13)	123.66(7)
O(1)-La(1)-O(13)	103.21(7)
O(2W)-La(1)-O(13)	127.81(7)
O(25)-La(1)-O(13)	122.45(6)
O(14)-La(1)-O(13)	47.63(6)
O(1W)-La(1)-O(13)	65.94(7)
O(7)-La(1)-O(26)	64.73(7)
O(1)-La(1)-O(26)	66.66(7)
O(2W)-La(1)-O(26)	63.43(7)
O(25)-La(1)-O(26)	47.05(6)
O(14)-La(1)-O(26)	131.33(6)
O(1W)-La(1)-O(26)	99.84(7)
O(13)-La(1)-O(26)	165.53(6)
O(32)-La(2)-O(26)	139.11(8)
O(2)-La(2)-O(20)	122.81(7)
O(3W)-La(2)-O(20)	63.03(7)
O(8)-La(2)-O(20)	130.02(6)
O(37)-La(2)-O(20)	102.50(7)
O(19)-La(2)-O(20)	47.10(6)
O(32)-La(2)-O(7)	105.13(7)
O(26)-La(2)-O(7)	64.98(7)
O(2)-La(2)-O(7)	66.99(7)
O(3W)-La(2)-O(7)	126.20(7)
O(8)-La(2)-O(7)	47.24(6)
O(37)-La(2)-O(7)	68.43(7)
O(19)-La(2)-O(7)	128.85(6)

O(20)-La(2)-O(7)	170.06(6)
O(32)-La(2)-O(2)	138.50(8)
O(26)-La(2)-O(2)	76.84(7)
O(32)-La(2)-O(3W)	127.66(7)
O(26)-La(2)-O(3W)	79.20(7)
O(2)-La(2)-O(3W)	66.67(8)
O(32)-La(2)-O(8)	70.82(8)
O(26)-La(2)-O(8)	112.19(7)
O(2)-La(2)-O(8)	76.17(8)
O(3W)-La(2)-O(8)	137.56(8)
O(32)-La(2)-O(37)	68.28(8)
O(26)-La(2)-O(37)	71.42(8)
O(2)-La(2)-O(37)	132.94(7)
O(3W)-La(2)-O(37)	136.09(8)
O(8)-La(2)-O(37)	84.63(8)
O(32)-La(2)-O(19)	85.06(8)
O(26)-La(2)-O(19)	74.80(7)
O(2)-La(2)-O(19)	132.85(8)
O(3W)-La(2)-O(19)	71.55(8)
O(8)-La(2)-O(19)	150.05(8)
O(37)-La(2)-O(19)	69.74(8)
O(32)-La(2)-O(20)	66.70(7)
O(26)-La(2)-O(20)	116.98(7)
Complex 8	
O(1)-Eu(1)	2.393(3)
O(7)-Eu(1)	2.522(4)
O(8)-Eu(1)	2.755(4)
O(14)-Eu(1)	2.359(4)
O(1W)-Eu(1)	2.393(4)
O(2W)-Eu(1)	2.396(4)
O(3W)-Eu(1)	2.461(4)
O(14)-Eu(1)-O(1W)	73.27(17)
O(14)-Eu(1)-O(1)	135.03(14)
O(1W)-Eu(1)-O(1)	139.94(15)
O(14)-Eu(1)-O(2W)	104.1(2)
O(1W)-Eu(1)-O(2W)	71.49(16)
O(1)-Eu(1)-O(2W)	73.58(15)
O(14)-Eu(1)-O(3W)	66.64(15)
O(1W)-Eu(1)-O(3W)	116.23(19)
O(1)-Eu(1)-O(3W)	70.10(14)

O(2W)-Eu(1)-O(3W)	72.86(17)
O(14)-Eu(1)-O(7)	142.64(15)
O(1W)-Eu(1)-O(7)	70.73(16)
O(1)-Eu(1)-O(7)	81.13(14)
O(2W)-Eu(1)-O(7)	73.56(16)
O(3W)-Eu(1)-O(7)	140.60(15)
O(14)-Eu(1)-O(8)	141.50(15)
O(1W)-Eu(1)-O(8)	108.61(15)
O(1)-Eu(1)-O(8)	68.36(12)
O(2W)-Eu(1)-O(8)	112.97(16)
O(3W)-Eu(1)-O(8)	133.68(14)
O(7)-Eu(1)-O(8)	48.12(12)

Complex 9

O(2)-Gd(1)	2.3888(13)
O(7)-Gd(1)	2.3520(15)
O(13)-Gd(1)	2.5139(14)
O(14)-Gd(1)	2.7702(15)
O(1W)-Gd(1)	2.4008(14)
O(2W)-Gd(1)	2.3959(15)
O(3W)-Gd(1)	2.4489(15)
O(7)-Gd(1)-O(2)	135.15(5)
O(7)-Gd(1)-O(2W)	73.18(6)
O(2)-Gd(1)-O(2W)	140.11(5)
O(7)-Gd(1)-O(1W)	104.25(7)
O(2)-Gd(1)-O(1W)	73.88(5)
O(2W)-Gd(1)-O(1W)	71.33(6)
O(7)-Gd(1)-O(3W)	67.03(5)
O(2)-Gd(1)-O(3W)	69.95(5)
O(2W)-Gd(1)-O(3W)	116.17(7)
O(1W)-Gd(1)-O(3W)	72.73(6)
O(7)-Gd(1)-O(13)	142.33(5)
O(2)-Gd(1)-O(13)	81.45(5)
O(2W)-Gd(1)-O(13)	70.65(6)
O(1W)-Gd(1)-O(13)	73.77(6)
O(3W)-Gd(1)-O(13)	140.66(5)
O(7)-Gd(1)-O(14)	141.22(5)
O(2)-Gd(1)-O(14)	68.13(4)
O(2W)-Gd(1)-O(14)	108.96(5)
O(1W)-Gd(1)-O(14)	113.16(6)

O(3W)-Gd(1)-O(14)	133.35(5)
O(13)-Gd(1)-O(14)	48.33(4)

Complex 10

O(1)-Gd(1)	2.5093(18)
O(2)-Gd(1)	2.4839(16)
O(7)-Gd(1)	2.4280(17)
O(8)-Gd(1)	2.4847(17)
O(9)-Gd(1)	2.5850(17)
O(10)-Gd(1)	2.4664(17)
O(1W)-Gd(1)	2.3678(16)
O(2W)-Gd(1)	2.3629(17)
O(2W)-Gd(1)-O(1W)	86.27(6)
O(2W)-Gd(1)-O(7)	145.09(6)
O(1W)-Gd(1)-O(7)	126.65(6)
O(2W)-Gd(1)-O(10)	78.62(7)
O(1W)-Gd(1)-O(10)	72.88(6)
O(7)-Gd(1)-O(10)	98.69(6)
O(2W)-Gd(1)-O(2)	74.30(6)
O(1W)-Gd(1)-O(2)	72.40(6)
O(7)-Gd(1)-O(2)	122.58(6)
O(10)-Gd(1)-O(2)	136.83(6)
O(2W)-Gd(1)-O(8)	147.94(6)
O(1W)-Gd(1)-O(8)	75.36(6)
O(7)-Gd(1)-O(8)	52.95(5)
O(10)-Gd(1)-O(8)	71.01(6)
O(2)-Gd(1)-O(8)	122.58(6)
O(2W)-Gd(1)-O(1)	126.68(6)
O(1W)-Gd(1)-O(1)	80.91(6)
O(7)-Gd(1)-O(1)	75.74(6)
O(10)-Gd(1)-O(1)	142.37(6)
O(2)-Gd(1)-O(1)	52.46(5)
O(8)-Gd(1)-O(1)	76.62(6)
O(2W)-Gd(1)-O(9)	77.43(6)
O(1W)-Gd(1)-O(9)	123.61(6)
O(7)-Gd(1)-O(9)	74.31(6)
O(10)-Gd(1)-O(9)	51.17(5)
O(2)-Gd(1)-O(9)	146.37(5)
O(8)-Gd(1)-O(9)	91.00(5)
O(1)-Gd (1)-O(9)	149.17(5)

Table S4. Best fitted parameters (χ_T, χ_S, τ and α) with the extended Debye model for **1** at 2 kOe in the temperature range 2-5.5 K.

T / K	χ_T / cm^3 mol^{-1}	χ_S / cm^3 mol^{-1}	α	τ / s	R²
2	0.27946	0.02985	0.21233	0.01715	0.9994
2.2	0.25665	0.02781	0.20627	0.01386	0.99938
2.4	0.23876	0.02584	0.20874	0.01111	0.99595
2.6	0.21821	0.02545	0.20394	0.00859	0.99688
2.8	0.20312	0.02188	0.19521	0.00638	0.99604
3	0.18624	0.02421	0.15463	0.00488	0.99641
3.5	0.15928	0.02416	0.09371	0.00226	0.99648
4	0.14029	0.02336	0.06349	9.30E-04	0.99806
4.5	0.12639	0.00519	0.06569	3.37E-04	0.99874
5	0.11431	0.03046	-0.03036	2.00E-04	0.99958
5.5	0.10465	0.03335	-0.04992	9.95E-05	0.99936

Table S5. Best fitted parameters (χ_T, χ_S, τ and α) with the extended Debye model for **3** at 3.5 kOe in the temperature range 2-5 K.

T / K	χ_T / cm^3 mol^{-1}	χ_S / cm^3 mol^{-1}	α	τ / s	R²
2	0.33078	0.01304	0.33891	0.00281	0.99901
2.2	0.30505	0.01184	0.33875	0.00242	0.99883
2.4	0.28053	0.01204	0.3256	0.00202	0.99914
2.6	0.26119	0.01275	0.30918	0.00169	0.99925
2.8	0.2436	0.01251	0.2885	0.00141	0.99948
3	0.22902	0.01247	0.28341	0.0012	0.99947
3.5	0.19918	0.01363	0.24809	7.79E-04	0.9998
4	0.17606	0.01614	0.19368	4.58E-04	0.9999
4.5	0.15816	0.01417	0.13373	2.46E-04	0.99989
5	0.14309	0.02573	0.06158	1.44E-04	0.99991